Heavy precipitation-induced Yangtze River runoff greatly regulates heterotrophic prokaryotes production and induces P-limited growth in the northern East China Sea

Yong-Jae Baek[1,2,3], Bomina Kim[1,4], Seok-Hyun Youn[5], Sang-Heon Lee[6], Hyo-Keun Jang[5,6], Heejun Han[3], Hugh W. Ducklow[7], Sung-Han Kim[2,3] and Jung-Ho Hyun[1*]

[1]Department of Marine Science & Convergence Technology, Hanyang University (ERICA), 55 Hanyangdaehak-ro, Sangnok-gu, Ansan, Gyeonggi-do 15588, Republic of Korea
[2]Department of Convergence Study on the Ocean Science and Technology, Ocean Science and Technology School, Busan 49111, Republic of Korea
[3]Marine Environmental Research Department, Korea Institute of Ocean Science and Technology, Busan 49111, Republic of Korea
[4]Southeast Sea Fisheries Research Institute, National Institute of Fisheries Science, Tongyeong 53085, Republic of Korea
[5]Oceanic Climate & Ecology Research Division, National Institute of Fisheries Science, Busan 46083, Republic of Korea
[6]Department of Oceanography and Marine Research Institute, Pusan National University, Busan 46241, Republic of Korea
[7]Department of Earth and Environmental Sciences and Lamont-Doherty Earth Observatory, Columbia University, Palisades, NY 10964, USA.

Correspondence to: Jung-Ho Hyun (hyunjh@hanyang.ac.kr)

Abstract. Although heterotrophic prokaryotes (HP) play a crucial role in biogeochemical carbon cycles, microbial oceanographic studies associated with heavy precipitation-induced large-scale freshwater runoff are understudied in the East China Sea (ECS), the largest continental shelf in the northwest Pacific. To elucidate the impact of Yangtze River diluted water (YRDW) on HP production (HPP) and growth-limiting resources, we conducted comprehensive microbial oceanographic measurements in combination with analysis of satellite images and optical property analyses of dissolved organic carbon (DOC) over three consecutive years in the northern ECS. Our results revealed that the HPP and chlorophyll-*a* were consistently highest in summer due to the supply of excess DOC and nutrients via YRDW, which is intriguing considering the enhanced HPP coupled with spring phytoplankton bloom in middle latitudes in general. However, the exceptionally great YRDW runoff induced by heavy rainfall resulted in excessive supply of terrestrial-origin recalcitrant DOC and nutrients imbalance with high N:P ratio (34), which was responsible for the limited DOC bioavailability and phosphorus-limitation for the HPP. Accordingly, the enhanced HPP-to-primary production ratio (> 0.5) in summer may suggest enhanced carbon flow via microbial food web, potentially altering food-web structure and energy transfer efficiency. Our results, demonstrating that YRDW can either stimulate or suppress HPP, provide new insights into microbial responses to large-scale freshwater discharge, which may be relevant to systems influenced by substantial freshwater inputs (e.g., Amazon River and Arctic Ocean).

1. Introduction

Due to the large quantity of dissolved organic carbon (DOC) in the ocean (~660 Pg), that is comparable to the amount of atmospheric CO_2, and its wide spectrum of reactivity, it is important to understand factors controlling oceanic DOC that ultimately regulates carbon storage in the ocean (Carlson and Hansell, 2015; Dittmar et al., 2021). With their high biomass and diverse metabolic functional genes (Ferrera et al., 2015; Bar-On and Milo, 2019), heterotrophic prokaryotes (HP) are a significant biological agent controlling the dynamics of DOC and inorganic nutrients in marine environments by: (1) transferring DOC from various sources to higher trophic levels (i.e. protozoa and microzooplankton) via the microbial loop, (2) mineralizing DOC to CO_2 via respiration, and (3) producing and sequestering recalcitrant DOC in the deep ocean via the microbial carbon pump (Azam et al., 1983; del Giorgio et al., 1997; Jiao et al., 2010). Therefore, quantifying HP parameters (i.e., biomass, production and respiration) and elucidating its controlling factors are fundamental steps in microbial oceanography which combines marine microbiology and microbial ecology with oceanography to elucidate the role of microorganisms in the biogeochemical element cycles in marine ecosystems (Ducklow and Carlson, 1992; Karl, 2007). Of all the controlling factors, hydrographic conditions that determine the physical structures and trophic status of the water column primarily regulate the distributions and metabolic activities of the bacterioplankton, which ultimately control the importance of the microbial loop in food web processes and biogeochemical carbon cycles in the water column (Hyun et al., 2005, 2009, 2016; Mann and Lazier, 2005; Baltar et al., 2007; Min et al., 2022).

The East China Sea (ECS) is the largest continental shelf (1.25×10^6 km^2) in the northwest Pacific Ocean (Supplement Fig. S1). In the ECS, several water masses, such as Taiwan warm current (TWC), Tsushima warm water (TWW), and Yangtze River diluted water (YRDW), prevail with seasonality (Lie and Cho, 2016; Seo et al., 2022). Relative significance of each current system largely determines physico-chemical and biological oceanographic properties of the ECS (Yoon et al., 2015). In particular, the YRDW flowing into the ECS in summer supplies substantial amounts of DOC (1.85 Tg C yr^{-1}), together with nitrogen and phosphorus (total nitrogen; 1.69 Tg N yr^{-1}, total phosphorus; 0.11 Tg P yr^{-1}) to the ECS (Shi et al., 2016; Wang et al., 2019). In addition, the construction of the Three-Gorges Dam on the upstream of the Yangtze River in 2006 has greatly altered the nutrient ratio in the YRDW. The mean N:P ratio in the northern ECS (nECS) increased from 22±18 during 2002-2009 to 97±64 during 2011-2022, which implied that growth of planktonic communities is likely to be limited by P-limitation (Supplement Fig. S2C, https://www.nifs.go.kr/kodc/soo_list.kodc, last access: 05 November 2024). Therefore, this long-term increase in N:P ratio (i.e., nutrient imbalance) along with high DOC and inorganic nutrients input via the runoff of YRDW raises fundamental ecological questions that HP growth in the ECS is either stimulated by the inputs of DOC or limited by phosphorus (P) in summer. Depending on whether HP growth is stimulated by DOC supply or suppressed by P-deficiency, the dynamics of carbon and nutrients and the structure of microbial communities are greatly affected (Obernosterer et al., 2003). So far, most microbial ecological and biogeochemical research in the ECS has predominantly focused on the southern part of the ECS (Shiah et al., 2003; Chen et al., 2009, 2021). Except for a few studies with limited spatial and temporal scales (< 1 year) (Zhao et al., 2010; Chen et al., 2014), little is known about the impact of YRDW on heterotrophic prokaryotes production

(HPP) and its interaction with DOC and inorganic nutrients in the nECS that serves as the main passage delivering organic carbon and nutrients directly from the Yangtze River and the South China Sea to the adjacent East Sea (Supplement Fig. S1, Lie and Cho, 2016; Nam et al., 2022).

One of the fundamental aims of microbial oceanography is to elucidate how the balance between HPP and primary production (PP) shapes the structure of marine food webs (Berglund et al., 2007). Since PP serves as the major organic carbon source for HP, the HPP:PP ratio of 0.15 in open ocean ecosystems, meaning that about 15% of PP supports HPP, indicates a tight coupling between HP and phytoplankton (Ducklow, 2000). However, in coastal systems, the HPP:PP ratios often exceed 0.6 and even surpass 1.0, indicating that HPP is no longer sustained solely by autochthonous organic carbon from phytoplankton production (Kim et al., 2020; Fernandes and Bogati, 2022). Such high HPP:PP ratios (i.e., uncoupling between HP and phytoplankton) suggest the increasing contribution of allochthonous organic carbon, such as terrestrial inputs (Kim et al., 2020). Under these conditions, the microbial loop becomes more dominant carbon flow, resulting in reduced food web efficiency with more trophic steps (Gasol et al., 1997; Straile, 1997; Joint et al., 2002), which can influence fish community structure and fisheries yield (Dickman et al., 2008). Given the gradual increase in freshwater input into the ECS, driven by global warming and intensifying East Asian monsoon rainfall (Qiao et al., 2024), understanding the balance between HPP and PP in the nECS is essential for assessing climate-driven changes in ecosystem functioning (Rowe et al., 2025).

Here, based on comprehensive microbial oceanographic studies, combining microbiological parameters with analysis of satellite images and optical properties of DOC, conducted seasonally for three consecutive years (2020–2022) in the nECS, we report two contrasting impacts of YRDW in regulating the HPP. First, owing to the combination of large riverine input of DOC and phytoplankton blooms fueled by nutrient supply from the YRDW, HPP was consistently enhanced in summer rather than in spring, which is anomalous for the mid-latitude regions in the northern hemisphere. Secondly, when the discharge of YRDW was excessive with exceptionally high recalcitrant DOC and high N:P (ca. 34), the HPP was regulated by limited DOC bioavailability and P-limitation. Considering the increasing frequency and intensity of heavy rainfall associated with climate change in the East Asian marginal seas (Fujibe et al., 2006; Li et al., 2019b), our results showing that different responses of HPP related to the strength of the YRDW provide significant information: (1) to interpret the role of microbial loop in microbial food web processes, and (2) to predict its future variations resulting from continued expansion of the YRDW in the East Asian marginal seas, one of the most rapidly changing oceanic environments due to anthropogenic activities and climate change-induced precipitation and warming (Fujibe et al., 2006; Belkin, 2009).

2. Materials and methods

2.1 Study area

As the largest continental shelf in the northwest Pacific Ocean (i.e., east Asian marginal seas), the ECS plays a critical role as a significant carbon reservoir, absorbing atmospheric carbon dioxide at a rate of 2.0 – 3.0 mol m^{-2} yr^{-1} (Wang et al., 2000; Kim

et al., 2013a). It is also one of the most productive fishing grounds for mackerel (*Scomber japonicus*) and anchovy (*Engraulis japonica*) and serves as a spawning ground for the Japanese flying squid (*Todarodes pacificus*) (Rebstock and Kang, 2003; Kim et al., 2013b).

The ECS is a hydrographically dynamic system driven by the Kuroshio current and northeast Asian Monsoon (Supplement Fig. S1, Lie and Cho, 2016). Like other large marine ecosystems that receive a tremendous amount of freshwater such as the Amazon Estuary (~6300 km^3 yr^{-1}) and Arctic shelves (~2000 km^3 yr^{-1}), the ECS receives a large amount of freshwater annually (900 km^3 yr^{-1}), especially during the summer monsoon period, and exhibits comparable biogeochemical complexity due to intense riverine input, seasonal stratification, and anthropogenic pressures (Milliman and Farnsworth, 2013; Spielhagen and Bauch, 2015). Therefore, the ECS is not only important for its ecological and fisheries productivity but also serves as a large marine ecosystem laboratory for investigating microbial biogeochemical processes in continental shelf systems influenced by enhanced freshwater inputs associated with the increasing trend of extreme precipitation under climate change (Khadgarai et al., 2021; Qiao et al., 2024).

2.2 Physico-chemical parameters

2.2.1 Sampling and handling

Seawater samples were collected using Niskin bottles attached to a rosette sampler, seasonally (i.e., February, May, August and November) at 7 to 8 stations in the nECS, located between 31.5°N–32.5°N and 124.5°E–127.1°E (Fig. 1), aboard the R/V *Tamgu* 3 of the Korean National Institute of Fisheries Science. The sampling bottles were pre-washed with 10% HCl and rinsed with Milli-Q water. Temperature and salinity were measured onboard using a CTD (SBE 911; Seabird Electronics, USA) attached to a rosette sampler. Seawater samples were collected concurrently at the same sampling stations. DOC, fluorescent dissolved organic matter (FDOM), prokaryotes abundance (PA), and HPP were measured at designated water depths (0, 10, 20, 30, 50, 75, 100, and 120 m). Samples for measuring HPP and PP were additionally collected at depths corresponding to 30% and 1% of surface photosynthetically active radiation, determined from Secchi disk measurements. The 1% light depth was defined as the euphotic depth (see *Dataset_Water_column.csv*). This sampling design enabled direct comparison of HPP and PP.

DOC and FDOM samples were filtered through pre-rinsed syringe filters (GF/F, 0.7-μm pore size, Whatman). The filters were rinsed thoroughly three times with 30 mL of the samples before filtration. Filtered samples were then transferred into 20 mL glass ampoules and 40 mL amber glass vials (both from Wheaton, Millville, USA) for DOC and FDOM samples, respectively. FDOM samples were immediately stored at -24°C until analysis. For DOC samples acidified with 6 N HCl (30 μL, final pH = 2) to inhibit microbial activity. The ampoule openings were sealed with fire to prevent external contamination. Glass ampoules and vials were combusted at 500°C for 5 h before use.

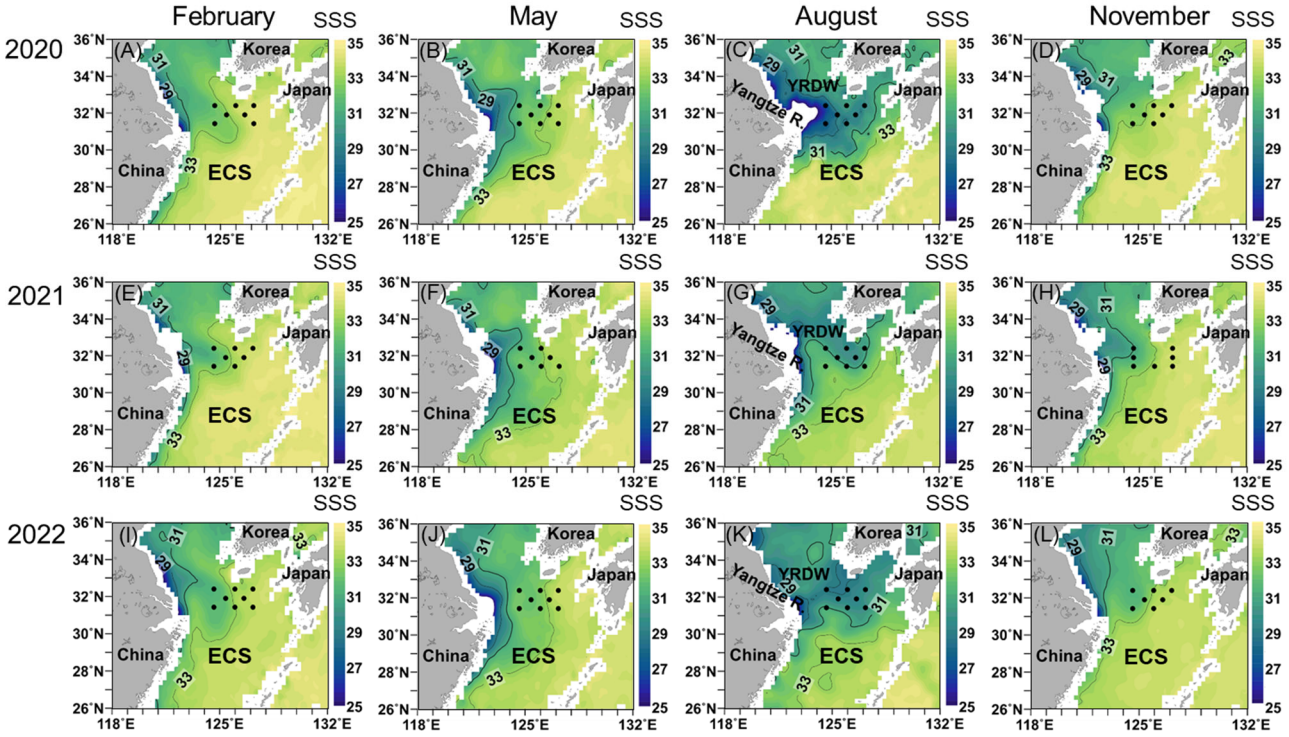

130 **Figure 1. Variations of sea surface salinity (SSS, psu) with season for three consecutive years (2020 - 2022) and sampling sites in the northern East China Sea (black dots). RSS SMAP Level 3 Sea Surface Salinity Standard Mapped Image Monthly V4.0 Validated Dataset was used from February 2020 to May 2022. JPL SMAP Level 3 CAP Sea Surface Salinity Standard Mapped Image 8-Day Running Mean V5.0 Validated Dataset was used from August 2022 to November 2022. The color bar indicates the salinity level.**

2.2.2 Laboratory analysis

Temperature–salinity (T–S) diagram analysis was conducted using 1 m bin-averaged T-S data (Fig. 2). For remote imagery on horizontal distribution of salinity, we adopted Level-3 Soil Moisture Active Passive (SMAP) Sea Surface Salinity (SSS) standard mapped images from 2020 to 2022, with a 0.25° horizontal resolution (Fig. 1).

DOC concentrations were determined using high-temperature catalytic oxidation (HTCO) with a TOC-L analyzer (Shimadzu, Japan). Instrument precision was assessed by measuring standard seawater samples (SSR; 71-75 μM DOC, University of Miami) every ten samples, with a precision of within 4%. The detection limit was confirmed as 3 μM through more than 10 measurements using Milli-Q water.

Excitation-emission matrix spectroscopy (EEMS) was performed using a Hitachi F-7100 spectrofluorometer (Hitachi, Tokyo, Japan) to characterize FDOM in seawater samples. Spectra were recorded with excitation wavelengths of 250–500 nm and emission wavelengths of 300–500 nm at 5 nm intervals. Fluorescence intensity was normalized to Raman units using Milli-Q water, and absorbance at 254 nm was confirmed to be <0.3 to avoid inner filter effects. A three-component PARAFAC model was constructed from 460 EEM spectra using the DOMFluor toolbox in MATLAB R2024a software (MathWorks Inc, Natick, USA), identifying one humic-like and two protein-like components (Coble, 1996; Stedmon and Bro, 2008). The humification index (HIX) was also calculated (Supplement Text S1). A detailed description of the EEM–PARAFAC procedure and component identification is presented in the Supplement Text S1. Concentrations of dissolved inorganic nitrogen (DIN, NO_2^- +NO_3^-), dissolved inorganic phosphorus (DIP), and chlorophyll-*a* (Chl-*a*) were obtained from the Korean National Institute of Fisheries Science. These data were collected during the same cruises aboard the R/V *Tamgu 3* (https://www.nifs.go.kr/kodc/soo_list.kodc, last access: 05 November 2024).

2.3 Microbiological parameters

2.3.1 Primary production

The PP was assessed using stable carbon isotope (^{13}C) analysis, following the methodology outlined by Hama et al. (1983). Water samples were obtained from six distinct photic depths, representing 100%, 50%, 30%, 12%, 5%, and 1% penetration of surface photosynthetically active radiation, determined through the conversion of Secchi disc depth measurements at each sampling station (see *Dataset_Light_penetration_depth.csv*). Samples were incubated under simulated in situ light and temperature conditions, and ^{13}C incorporation into particulate organic carbon was analyzed using isotope ratio mass spectrometry. A detailed description of incubation procedures, filtration, isotope analysis, and productivity calculation is provided in the Supplement Text S2.

2.3.2 Prokaryotes abundance

Samples for enumerating the PA were preserved with glutaraldehyde at a final concentration of 1% and stored in a freezer at – 20 °C (Hyun and Yang, 2003). The PA was measured using the DAPI-staining method (Porter and Feig, 1980). More than 20 microscopic fields were examined using an epifluorescence microscope (Nikon, Eclipse 80i) equipped with a mercury lamp (HB-10101 AF), an ultraviolet (UV) excitation filter, and a BA 420 barrier filter.

2.3.3 Heterotrophic prokaryotes production

The HPP was determined by measuring the incorporation of ^{3}H-leucine into protein, following the method of Smith and Azam (1992). Seawater samples (1.5 mL) were incubated with ^{3}H-leucine (final concentration, 10 nM, Perkin Elmer, NET1166005) at in situ temperature for one hour in the dark, and radioactivity in the synthesized protein was measured using a liquid scintillation counter (LKB, Rack Beta II). The calculated protein synthesis rate of ^{3}H-leu (pmol leu L^{-1} h^{-1}) was converted to HPP (μg C L^{-1} d^{-1}) using a conversion factor (CF = 1.5 kg C mol $leucine^{-1}$; Kirchman, 1993). A detailed description of incubation, extraction, and counting procedures is presented in the Supplement Text S3.

2.3.4 HP growth limiting resources assay

To investigate the limiting resources for HP growth in different water masses, factorial nutrient addition bioassays (Rivkin and Anderson, 1997) were conducted in the nECS and the East Sea sites on 16 August 2020 and 11 August 2020, respectively, and additionally on 27 April 2021 in the nECS site. Seawater samples were collected at a depth of 10 m at each site, and filtered through polycarbonate filter (0.2 μm pore size) to remove protozoan grazers (Kim et al., 2025). The filtered water was mixed with unfiltered seawater at a 9:1 ratio in one-liter polycarbonate bottles to minimize bottle effects while maintaining the natural bacterial assemblage (Ferguson et al., 1984). Glucose (final concentration, 10 μM) as organic C source, NH_4Cl (final concentration, 3 μM) as N source, and NaH_2PO_4 (final concentration, 1 μM) as P source were added alone or in combination (i.e., unamended control, +C, +N, +P, +CN, +CP and +NP). The bottles were incubated in a non-transparent on-deck incubator with circulating sea surface water during the incubation period. Subsamples for measuring HPP were collected in triplicate after 12 h incubation in August 2020 and 26.5 h in April 2021. The longer incubation time in April 2021 was chosen to account for lower spring temperatures that could delay microbial metabolic responses (Table 2). Subsampling for the initial HPP was conducted on the unamended control bottle.

2.4 Data analysis and statistics

The mixed layer depth (MLD) was defined as the depth immediately above the onset of the thermocline. The euphotic depth was determined based on Lambert–Beer's law described in Poole and Atkins (1929) using a Secchi disk. The Riemann sum method was applied to integrate the parameters within the mixed layer and euphotic depths. Statistical analyses were conducted

using IBM SPSS Statistics 27. Detailed descriptions of statistical procedures are presented in Supplement Text S4. Abbreviations used in the main text and figures are provided in Table S4 in the Supplement.

3. Results

3.1 Hydrographic conditions

Based on T-S diagrams, the current systems in the study area were defined by 2-4 water masses that vary seasonally (Fig. 2). The two main currents appearing in the nECS are the Kuroshio Source Water and the Shelf Mixed Water (Fig. 2). The Kuroshio Source Water is formed by the convergence of the TWC and the TWW, which are both branches of the main Kuroshio Current in the nECS and are characterized by high temperature and salinity (Supplement Fig. S1). In contrast, the Shelf Mixed Water is formed by the mixing of the Kuroshio Source Water with the Chinese Coastal Current. The Chinese Coastal Current, which is mainly observed on the shelf side of the East China Sea, is characterized by cold and low-salinity properties (Li et al., 2006). As a result, the Shelf Mixed Water exhibits relatively lower temperature and salinity due to the influence of the Chinese Coastal Current. During February (winter), May (spring), and November (autumn), the nECS consisted of Kuroshio Source Water and Shelf Mixed Water (Fig. 2A, B, D, E, F, H, I, J, L; Supplement Table S1). However, during August (summer), a more complex water mass distribution was observed due to strong stratification and substantial freshwater input: TWC and YRDW were present near the surface, whereas TWW and Shelf Mixed Water were observed in the mid to lower layers, which differed from other seasons (Fig. 2C, G, K; Supplement Table S1). The satellite images of sea surface salinity (Fig. 1), together with the T-S diagrams (Fig. 2), clearly revealed that YRDW (< 31 psu, the blue-green colors in Fig. 1C, G, K) originating from the Yangtze River in August expands northeastward to the nECS located approximately 300 km away from the Yangtze River estuary. The expansion of YRDW to the nECS was greatest in August 2020, followed by August 2022 and 2021, respectively (Fig. 1; Fig. 2).

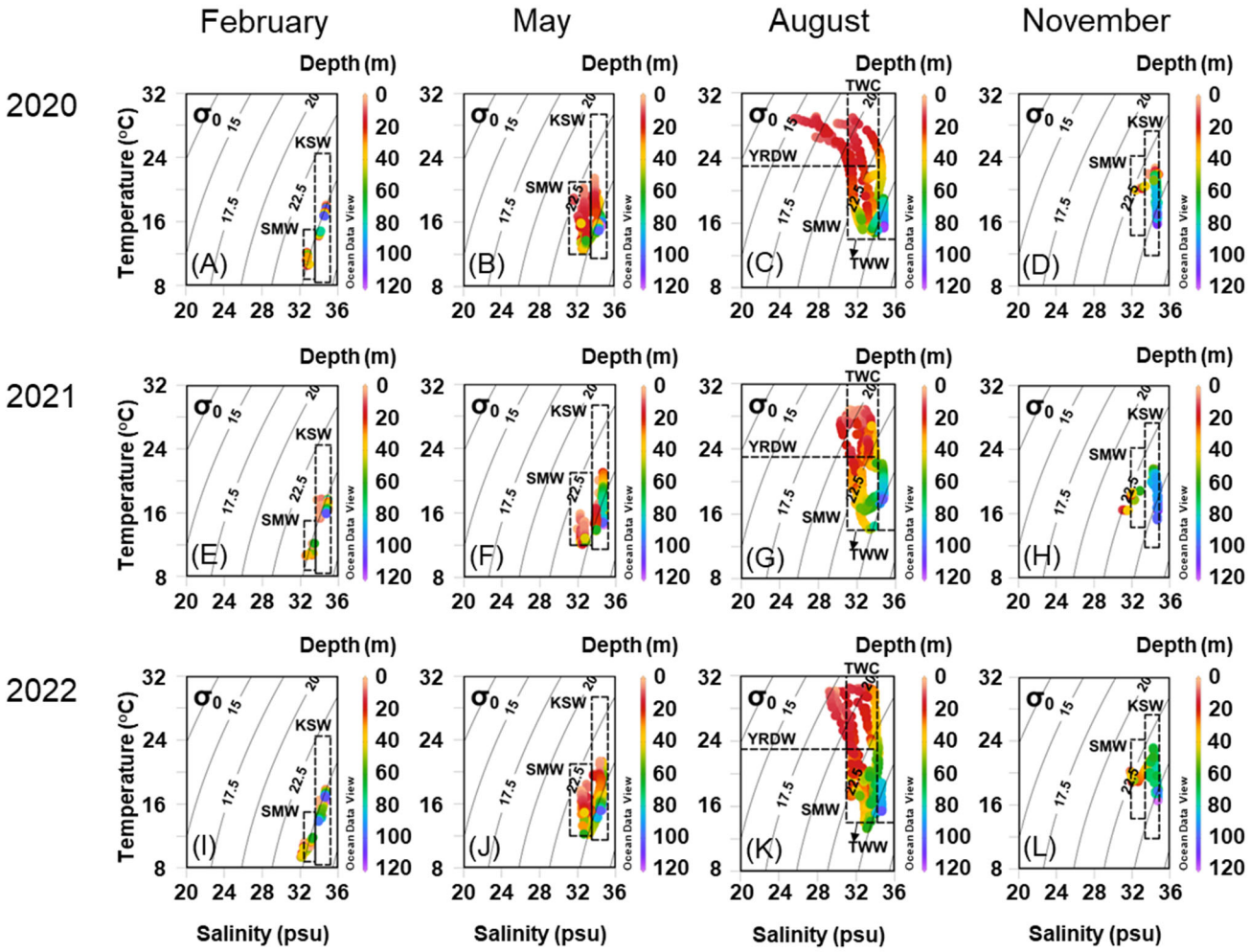

Figure 2. Seasonal T-S diagrams of the East China Sea (ECS) in 2020 (A, B, C, D), 2021 (E, F, G, H), and 2022 (I, J, K, L). The dashed box indicates the defined water masses in this study observed in the northern ECS (Gong et al., 1996; Hur et al., 1999; Kim and Youn, 2023). Grey contour lines represent the sigma-t. The color bar indicates the depth of the water column. KSW: Kuroshio source water, SMW: Shelf mixed water, YRDW: Yangtze River diluted water, TWW: Tsushima warm water, TWC: Taiwan warm current.

3.2 DOC, Chl-*a* and primary production

The vertical distributions of DOC reflected seasonal changes in water column structure (Fig. 3). In February and November, DOC concentrations were relatively homogeneous within the MLD (50–70 m), averaging 65 ± 2 μM (53 – 76 μM) and 64 ± 2 μM (55 – 83 μM), respectively (Fig. 3C, W). In contrast, during May and August, DOC concentrations increased with decreasing MLD, averaging 72 ± 1 μM (66 – 74 μM) in May and 86 ± 3 μM (75 – 130 μM) in August (Fig. 3K, Q; Table 1). Elevated DOC concentrations were particularly evident in August within the low-salinity surface layer (upper 10 m), where values averaged 95 ± 19 μM (76–130 μM; Fig. 3P, Q). Among the summer observations, August 2020 exhibited the highest DOC concentrations (104 ± 5 μM), which were significantly higher than those in August 2021 and 2022 (77 ± 1 μM and 80 ± 3 μM, respectively; $p = 0.002$), coinciding with the strongest influence of YRDW observed during the study period (Fig. 1C, 4A). Chl-*a* concentrations within the MLD followed a similar pattern: homogeneously low in February (0.47 ± 0.02 μg L^{-1}; 0.42 – 0.49 μg L^{-1}), increasing in May (1.05 ± 0.24 μg L^{-1}; 0.77 – 1.22 μg L^{-1}) with the development of thermal stratification, remaining elevated in August (avg. 0.74 ± 0.22 μg L^{-1}; 0.58 – 0.99 μg L^{-1}) under strong haline stratification associated with YRDW intrusion, and decreased in November (avg. 0.53 ± 0.02 μg L^{-1}; 0.50 – 0.55 μg L^{-1}) (Fig. 3I, P, L, R).

PP, integrated over the euphotic depth, followed a similar seasonal pattern, increasing from May to August and peaking at 336 ± 55 mg C m^{-2} d^{-1} (August 2021) and 263 ± 73 mg C m^{-2} d^{-1} (August 2022) (Fig. 4D). Notably, PP in August 2020 (182 ± 77 mg C m^{-2} d^{-1}) was significantly lower than other years ($p = 0.028$) (Fig. 4D), despite high YRDW input.

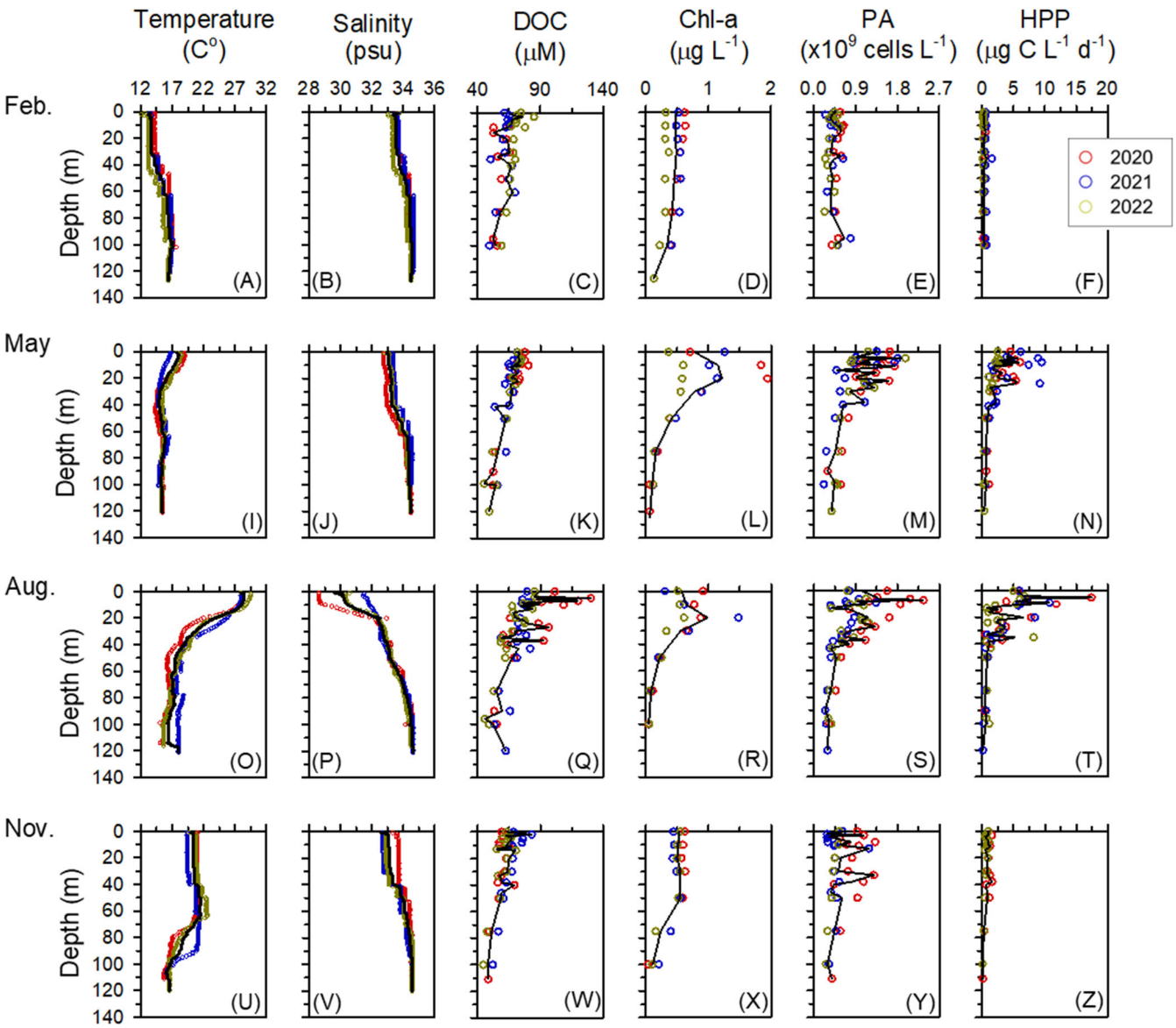

Figure 3. Vertical profiles of temperature, salinity, dissolved organic carbon (DOC), chlorophyll-*a* (Chl-*a*), heterotrophic prokaryotes abundance (PA), and heterotrophic prokaryotes production (HPP) in the northern East China Sea from 2020 to 2022. Each symbol represents the average value at a given depth from 7–8 stations sampled during each survey, and the solid black line denotes the mean of the three-year averages.

Table 1. Seasonal averages (± 1 SE) of microbial oceanographic parameters in the northern East China Sea from 2020 to 2022. Chlorophyll-*a* (Chl-*a*) and prokaryote abundance (PA) represent mean values within the euphotic zone, whereas primary production (PP) and heterotrophic prokaryotes production (HPP) represent values integrated over the euphotic zone. Physical and chemical variables (e.g., temperature, salinity, dissolved organic carbon) are averaged within the mixed layer depth.

Season	Water depth (m)	Euphotic depth (m)	Mixed layer depth (m)	Temp (°C)	Salinity (psu)	DOC (μM)	Chl-*a* (μg L^{-1})	PA ($\times 10^9$ cells L^{-1})	PP (mg C m^{-2} d^{-1})	HPP (mg C m^{-2} d^{-1})
Spring	80±28	23±8	16±10	18.1±2.1	33.1±0.9	72±1	0.75±0.13	1.28±0.09	216±26	84±13
Summer	77±29	31±8	14±6	28.3±1.1	30.4±1.9	86±3	0.75±0.11	0.99±0.09	264±40	168±25
Autumn	75±30	21±16	51±23	20.4±1.7	33.1±1.2	64±2	0.53±0.04	0.66±0.08	242±50	15±4
Winter	78±29	17±13	76±32	13.6±3	33.5±1	65±2	0.38±0.02	0.46±0.03	89±15	9±1

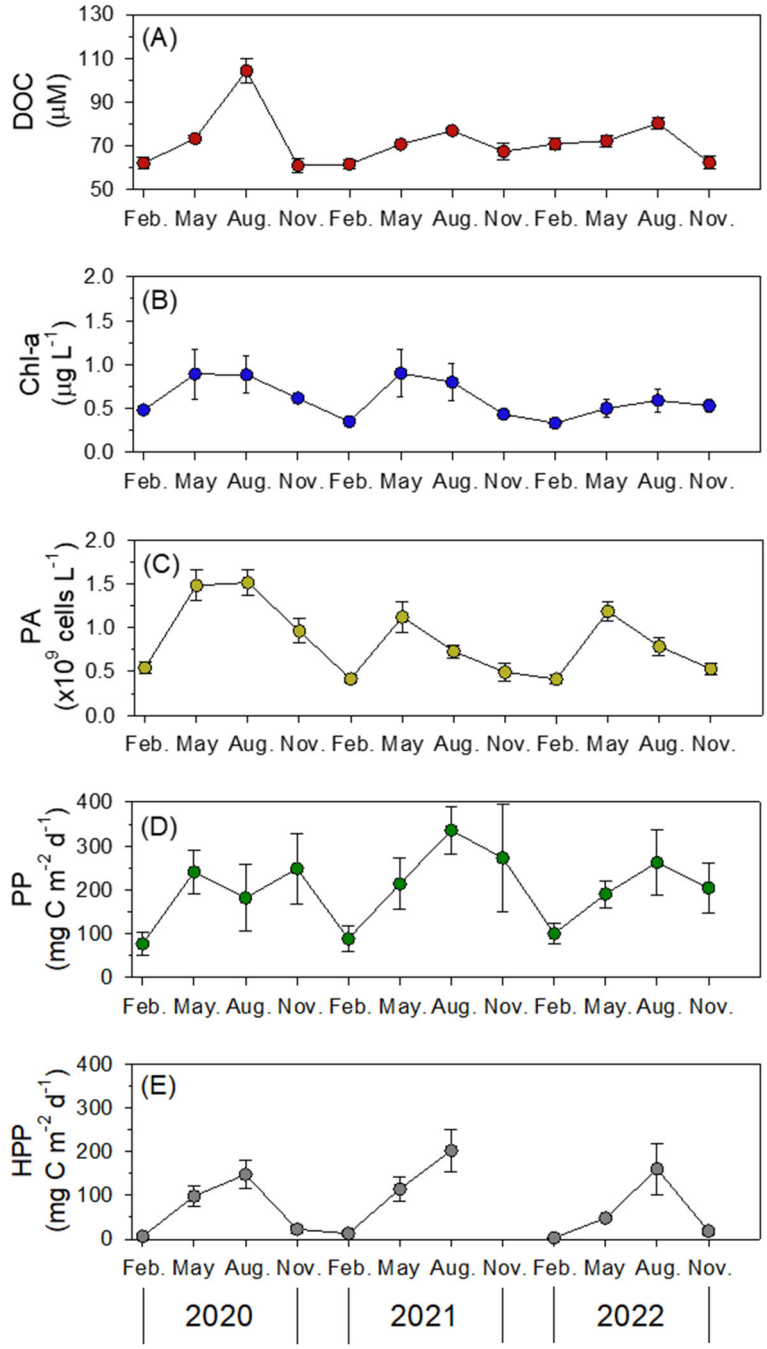

Figure 4. Seasonal variations of dissolved organic carbon (DOC) concentrations with values averaged to the mixed layer depth (A), chlorophyll-*a* (Chl-*a*) concentrations (B), and prokaryotes abundance (PA) (C) averaged within the euphotic depth, primary production (PP) (D), and heterotrophic prokaryotes production (HPP) (E) values integrated over the euphotic depth in the northern East China Sea. Error bars represent standard errors.

3.3 Prokaryotes abundance and heterotrophic prokaryotes production

Mean PA within the euphotic depth was lowest and vertically homogeneous in February ($0.46 \pm 0.03 \times 10^9$ cells L^{-1}; 0.35 – 0.59×10^9 cells L^{-1}). In contrast, PA reached its highest values in May ($1.28 \pm 0.09 \times 10^9$ cells L^{-1}; $0.48 – 1.88 \times 10^9$ cells L^{-1}), before declining in August ($0.99 \pm 0.09 \times 10^9$ cells L^{-1}; $0.37 – 2.36 \times 10^9$ cells L^{-1}) and November ($0.66 \pm 0.08 \times 10^9$ cells L^{-1}; $0.28 – 1.29 \times 10^9$ cells L^{-1}) (Fig. 3; Table 1). PA correlated positively with DOC ($\rho = 0.255$, $p < 0.001$) and Chl-*a* ($\rho = 0.281$, $p < 0.001$; Supplement Table S2).

HPP within the euphotic depth followed a seasonal cycle: lowest in February (0.33 ± 0.12 µg C L^{-1} d^{-1}; 0.20 – 0.58 µg C L^{-1} d^{-1}), rising in May (3.73 ± 1.37 µg C L^{-1} d^{-1}; 1.76 – 5.86 µg C L^{-1} d^{-1}), reaching a consistent summer peak in August (5.51 ± 4.08 µg C L^{-1} d^{-1}; 0.69 – 17.43 µg C L^{-1} d^{-1}), and then declining in November (0.83 ± 0.26 µg C L^{-1} d^{-1}; 0.43 – 1.24 µg C L^{-1} d^{-1}) (Fig. 3). HPP correlated positively with temperature ($\rho = 0.525$, $p < 0.001$), DOC ($\rho = 0.457$, $p < 0.001$) and Chl-*a* ($\rho = 0.398$, $p < 0.001$; Supplement Table S2) consistent with the observed summer peak.

4. Discussion

4.1 Exceptionally enhanced HPP in summer

In the present study, one of the most prominent features observed in oceanographic and microbiological properties was the consistent summer peak in HPP (Fig. 4E). Considering the typically enhanced HPP coupled with phytoplankton bloom in spring in the middle latitudes of the northern hemisphere (Amon and Benner, 1998; Lemée et al., 2002; Gomes et al., 2015), our results showing consistently high summer peaks in microbiological parameters are noteworthy. Plankton activities are positively correlated with temperature in many marine systems, a pattern that has been widely reported in previous studies (White et al., 1991; Robinson and Williams, 1993), suggesting that elevated summer temperatures may partially contribute to high HPP. However, assuming a Q_{10} of 2, a 10 ℃ temperature increase from 15 ℃ to 25 ℃ would yield an approximately twofold increase in HPP. In contrast, estimates from the observed seasonal temperature–HPP relationship suggest a fivefold increase from 28 to 140 mg C m^{-2} d^{-1} (Supplement Fig. S3), exceeding that expectation. In addition to temperature, positive correlations between HPP and DOC ($\rho = 0.457$, $p < 0.001$) and between HPP and Chl-*a* ($\rho = 0.398$, $p < 0.001$) indicate that these factors acted as co-drivers of the consistently elevated HPP observed in summer, coinciding with the expansion of YRDW (Fig. 1; Table 1; Supplement Table S2).

Since the expansion of YRDW in summer was the most notable observation in the nECS (Fig. 2), we further analyzed the impact of YRDW in regulating the HPP to better interpret the cause-effect relationship on the high HPP in summer. Firstly, the correlation analysis between salinity and DOC for three years (2020-2022) consistently revealed a significant negative relationship (Fig. 5A – C). Especially higher concentrations of DOC were observed in August with low salinity conditions (< 31 psu), which indicated a substantial input of DOC into the nECS via the inflow of YRDW. Secondly, the HPP showed a significantly positive relationship with DOC in the summer of all three years, which suggested that the high HPP in summer is greatly stimulated by the DOC supply (Fig. 5D–F). Moreover, the three-year pooled summer Chl-*a* data also showed a significant correlation with HPP, indicating the combined effect of DOC from terrestrial and phytoplankton sources (Fig. 6A). Consequently, these correlation analyses between salinity-DOC-HPP, along with the tight coupling between Chl-*a* and HPP, clearly demonstrated that the high HPP in summer is intrinsically stimulated by the input of DOC-rich YRDW and enhanced summer phytoplankton bloom driven by nutrient input (Fig. 5, 6A). Similar findings have been reported in the southern ECS (25.4 – 31.6 ºN, 120.5 – 127.0 ºE), where HPP in the euphotic depth was highest during the summer months, coinciding with the wider distribution of YRDW in summer periods (Shiah et al., 2003; Chen et al., 2009, 2021). Our results, combining extensive satellite images analyses, variations of hydrographic conditions, concentrations of DOC and Chl-*a*, and HPP variations with season, provide comprehensive and direct evidence on the impact of YRDW in stimulating consistently high HPP in summer.

Recent climate modeling studies suggest that the intensity of precipitation in East Asia during summer monsoon period will be increasing with global warming (Li et al., 2019b, Khadgarai et al., 2021; Qiao et al., 2024). In this regard, the high HPP in summer in the nECS has a significant ecological implication to the microbial oceanography of the adjacent seas (i.e., Yellow Sea and East Sea) where high HPP still prevails in spring. To investigate further the potential impact of YRDW on HPP in summer in the adjacent seas, we assembled available HPP data: (1) from the East Sea that is affected by the intrusion of YRDW in summer, and (2) from the Yellow Sea, relatively less affected by the YRDW (Supplement Fig. S1, 5). Indeed, the average HPP in summer (62 ± 72 mg C m^{-2} d^{-1}) of the East Sea was not significantly different from that measured in spring (77 ± 94 mg C m^{-2} d^{-1}) (Supplement Fig. S5B, $p = 0.518$). This relationship suggests that the YRDW directly flowing into the East Sea via nECS (Chang and Isobe, 2003) stimulates the HPP in summer. In contrast, the average HPP in summer (22 ± 9 mg C m^{-2} d^{-1}) of the Yellow Sea remained significantly lower than that measured in spring (75 ± 58 mg C m^{-2} d^{-1}) (Supplement Fig. S5C, $p < 0.001$). Our findings of elevated HPP in summer of the nECS and the East Sea highlight the importance of sustained ecological monitoring to better understand the extensive influence of climate change-induced precipitation on the HPP in the nECS and its adjacent seas (Chen et al., 2021).

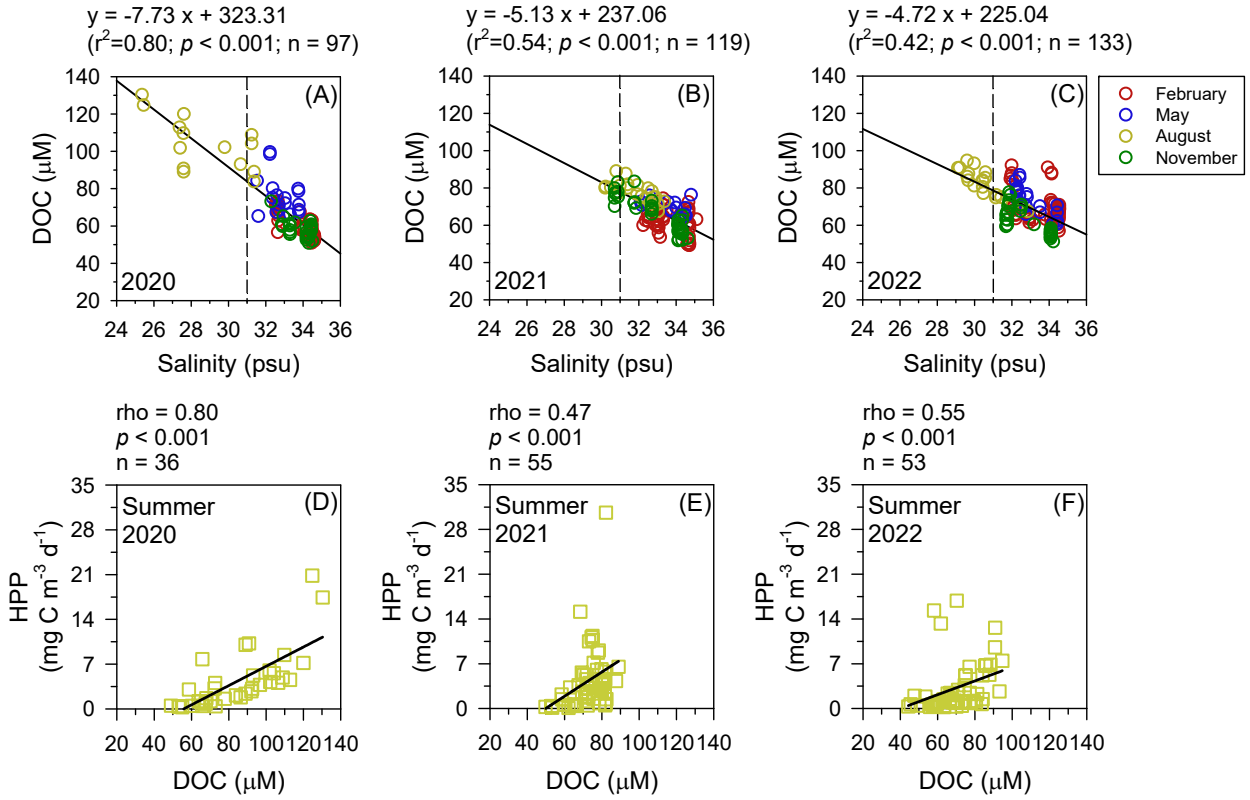

Figure 5. Interrelationships between salinity and dissolved organic carbon (DOC) (A, B, and C) within mixed layer depth in 2020, 2021 and 2022, and Spearman's correlation analysis between DOC and heterotrophic prokaryotes production (HPP) (D, E, and F) during the summers of 2020, 2021, and 2022 in the northern East China Sea. The dashed lines indicate a salinity < 31 psu, which represents the salinity of Yangtze River diluted water.

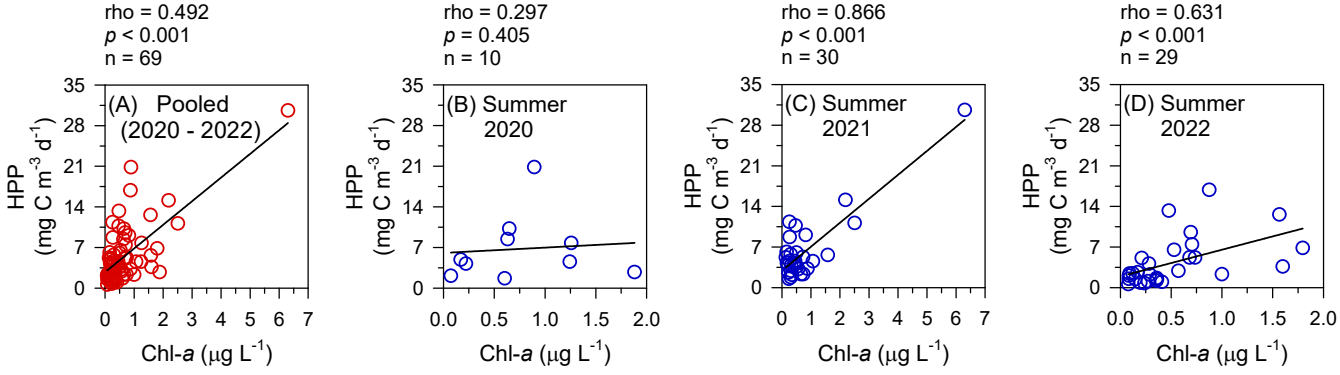

Figure 6. Relationships between Chl-*a* and heterotrophic prokaryotes production (HPP) within the euphotic depth in August of the three-year pooled data (A), 2020 (B), 2021 (C), 2022 (D) in the northern East China Sea. Spearman's rank correlation analysis was conducted for the pooled data (A), 2020 (B), and 2022 (D), while Pearson correlation analysis was applied to 2021 (C).

4.2 Suppression of HPP during greater YRDW intrusion

Despite the extraordinarily enhanced DOC input in August 2020 (Fig. 4A, 5A; Supplement Fig. S4A) resulting from the unusually heavy rainfall compared to that measured in August 2021 and 2022 (Fig. 1C, 2C, 4A), the HPP value in 2020 remained similar to that of 2021 and 2022 (Fig. 4E; Supplement Fig. S4B). This result suggests that a substantial fraction of the DOC transported to the nECS via YRDW in summer 2020 contained much more recalcitrant dissolved organic matter (DOM) for HP metabolism (Guo et al., 2014; Li et al., 2020; Chen et al., 2024). Indeed, the fluorescence intensity of the $FDOM_H$ (i.e., humic-like FDOM, Coble, 1996) was highest in the high DOC range (> 90 μM) (Fig. 7A) within the YRDW fraction (< 28 psu) (Fig. 7B) in August 2020. Consistent with this, the HIX, a proxy for the refractory nature of DOM (Hansen et al., 2016; Li et al., 2019a), also reached its highest level (1.79 ± 0.36) in August 2020 (Fig. 6C). HIX reflects the relative contribution of humic-like FDOM in the DOM pool, which is generally characterized by high aromaticity, molecular weight, and structural complexity (Hansen et al., 2016). Such humic-like FDOM are known to exhibit low biogeochemical reactivity and resistance to microbial degradation, resulting in their persistence in aquatic environments (Yamashita and Tanoue, 2008; Cao et al., 2019). Under these conditions, HP tend to utilize organic matter primarily for cell maintenance (i.e., for energy-yielding respiration) rather than for biomass synthesis (i.e., production) (Carlson et al., 2007; Fasching et al., 2014).

A plausible explanation for maintaining a low bioavailable DOC pool in August 2020 is the reduced PP observed during that period (Fig. 4D). The Yangtze River carries a large amount of sediment into the estuary (ca. 4.86×10^8 tons per year), making it one of the most turbid estuaries in the world (Guo et al., 2014). This high turbidity can result in limited photodegradation of humic substances in the Yangtze River Estuary (Li et al., 2015). The YRDW, which contains abundant terrestrial humic substances, can reach the nECS after passing through this highly disturbed area, driven by southeasterly winds (Supplement Fig. S1). The strong signals of $FDOM_H$ in August 2020, when YRDW input was greatest, suggest both elevated terrestrial input and limited photodegradation (Fig. 7B). This implies that a more turbid water plume reached the nECS in 2020 than in 2021 and 2022. Indeed, the average euphotic depth in August 2020 was only 26±4 m, compared to 33±6 m and 34±11 m in 2021 and 2022, respectively. This higher turbidity likely limited light penetration, resulting in reduced PP and a diminished supply of labile DOC (Huguet et al., 2009; Jiang et al., 2016). As a result, the DOM pool in August 2020 was characterized by a higher relative contribution of refractory DOC, as reflected in the elevated HIX values (Fig. 7C).

Consequently, although the intrusion of YRDW supplying a substantial amount of bioavailable DOC in summer significantly stimulates HPP (Fig. 5), exceptionally great YRDW input, as it was observed in August 2020 (Fig. 5A), likely altered DOC quality by oversupplying terrestrial recalcitrant DOM and reduced PP by limiting light availability in turbid water column, thereby limiting the additional stimulation of HPP (Fig. 4E).

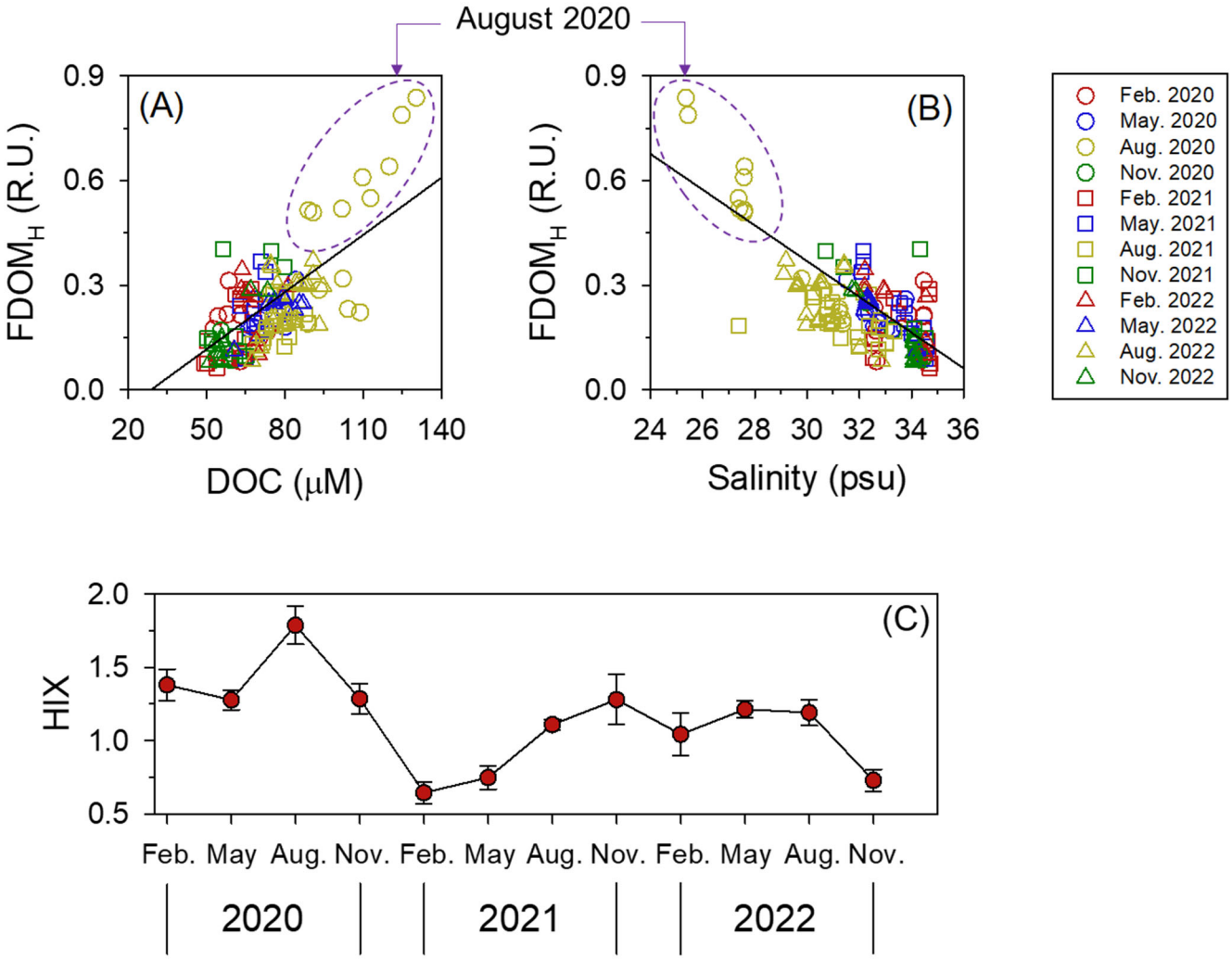

Figure 7. Relationships of dissolved organic carbon (DOC) and salinity with humic-like fluorescent dissolved organic matter ($FDOM_H$) (A and B), and the seasonal variations of the humification index (HIX) (C) within the mixed layer depth over three consecutive years across four seasons in the northern East China Sea. Error bars represent standard errors.

4.3 Impact of YRDW on phosphorus limited HPP

The Yangtze River has been reported to change the nutrient balance in the ECS by excessive DIN influx and relatively low DIP influx (Chen et al., 2020). In the turbid estuary, the DIP is generally removed by suspended particles (Lopez et al., 1996), which consequently triggers a nutrient imbalance (i.e., high N:P ratio) in the Yangtze River Estuary. In general, DOC is recognized as the major limiting substrate for HP growth in the ocean. However, since pico-sized prokaryotes have a high surface area-to-volume ratio that requires more phospholipids to make up cell membranes and contain higher nucleic acids (P-rich) fractions than phytoplankton on a per-cell basis, they have relatively high P demand for growth (Goldman et al., 1987; Fagerbakke et al., 1996). This frequently results in a P-limited growth of HP in various marine environments (Thingstad et al., 2005; Yuan et al., 2011).

To directly demonstrate the impact of YRDW in regulating HP growth, we conducted three incubation experiments under different DOC and P conditions (Fig. 8; Table 2). The first experiment was carried out in August 2020 at the nECS site (Fig. 8A; Exp. 1 in Table 2) where the hydrographic condition was characterized by the expansion of the YRDW with high N:P ratio (34) and exceptionally high DOC containing high humic-like FDOM (Fig. 7). The second experiment was conducted during the same summer as the first experiment in the East Sea where the water mass was dominated by the high T-S TWW with N:P ratio of 15.09 (Fig. 8B; Exp. 2 in Table 2). The HPP was stimulated in P-amended samples exclusively at the YRDW-prevailing nECS site (Fig. 8A), while HPP was stimulated in glucose amended samples at TWW-prevailing East Sea site (Fig. 8B). Considering the highest DOC concentration (91 μM) and an abnormally high N:P ratio (34) (Table 2), the results indicated that intrusion of P-depleted YRDW was primarily limiting the HPP in the nECS in summer (Fig. 8A; Table 2). Based on the two experiments, we further hypothesized that if YRDW is not prevailing in the nECS, the HPP is not likely to be limited by the P deficiency. To confirm the hypothesis, we conducted the third experiment at the nECS site in April 2021 when the water mass was dominated by the Kuroshio source current (TWW and TWC) with high salinity (Fig. 8C; Exp. 3 in Table 2). Indeed, the HPP was stimulated only in the samples amended by glucose (+C, +CN and +CP). Combining these three growth-limiting resource experiments conducted at different water regimes in time and space demonstrates that the HPP in the nECS is closely regulated by the hydrographic conditions varying with season. It is primarily limited by P availability in summer when YRDW prevails, whereas organic carbon limitation is more significant in other seasons when Kuroshio source current (TWC and TWW) dominates (Supplement Fig. S1).

This P deficiency may have also influenced phytoplankton composition and their production of bioavailable organic matter, ultimately affecting HPP. In August 2020, despite the tight coupling between HPP and DOC ($p < 0.001$, Fig. 5D), there was no significant correlation between HPP and Chl-*a* ($p = 0.405$, Fig. 6B), unlike the patterns observed in other years (Fig. 6C, D). This uncoupling between HPP and phytoplankton-derived organic matter suggests a possible shift toward smaller phytoplankton communities under P limitation (Fig. 6B). Previous studies in the ECS have reported that elevated N:P ratios associated with YRDW inputs can drive shifts in phytoplankton community structure, transitioning from larger diatom dominance to smaller phytoplankton such as cyanobacteria, small dinoflagellates, and cryptophytes that prefer environments

with low DIP availability (Gomes et al., 2018; Park et al., 2022). Such DIP limitation on phytoplankton growth may be further intensified by competition with HP that can be more efficient in acquiring phosphorus under high-DOC and low-P conditions driven by YRDW (Drakare, 2002). Moreover, exudates released from P-depleted phytoplankton tend to be less bioavailable for HP growth by supplying more recalcitrant organic carbon that is poorly suited for bacterial uptake (Kragh and Søndergaard, 2009; Puddu et al., 2003). Therefore, severe P deficiency induced by the excessive input of YRDW results in uncoupling between HPP and phytoplankton-derived organic matter (i.e. P-depleted exudates), leading HPP in August 2020 to rely primarily on terrestrial DOC (Fig. 5D).

Together with the refractory properties of the DOC and the reduced PP driven by high turbidity (Fig. 7), this P-limited HPP (Fig. 8A) and its uncoupling with phytoplankton (Fig. 6B) in August 2020 provide further evidence explaining why HPP was not so great even in summer 2020 with exceptionally high DOC compared to that measured in summer 2021 and 2022 (Fig. 4E). In a P-starved condition, HP is unable to synthesize nucleic acids, protein, and ATP, which limits their ability to replicate cells and metabolize (i.e., degrade and uptake) organic carbon (Obernosterer et al., 2003; Kritzberg et al., 2010).

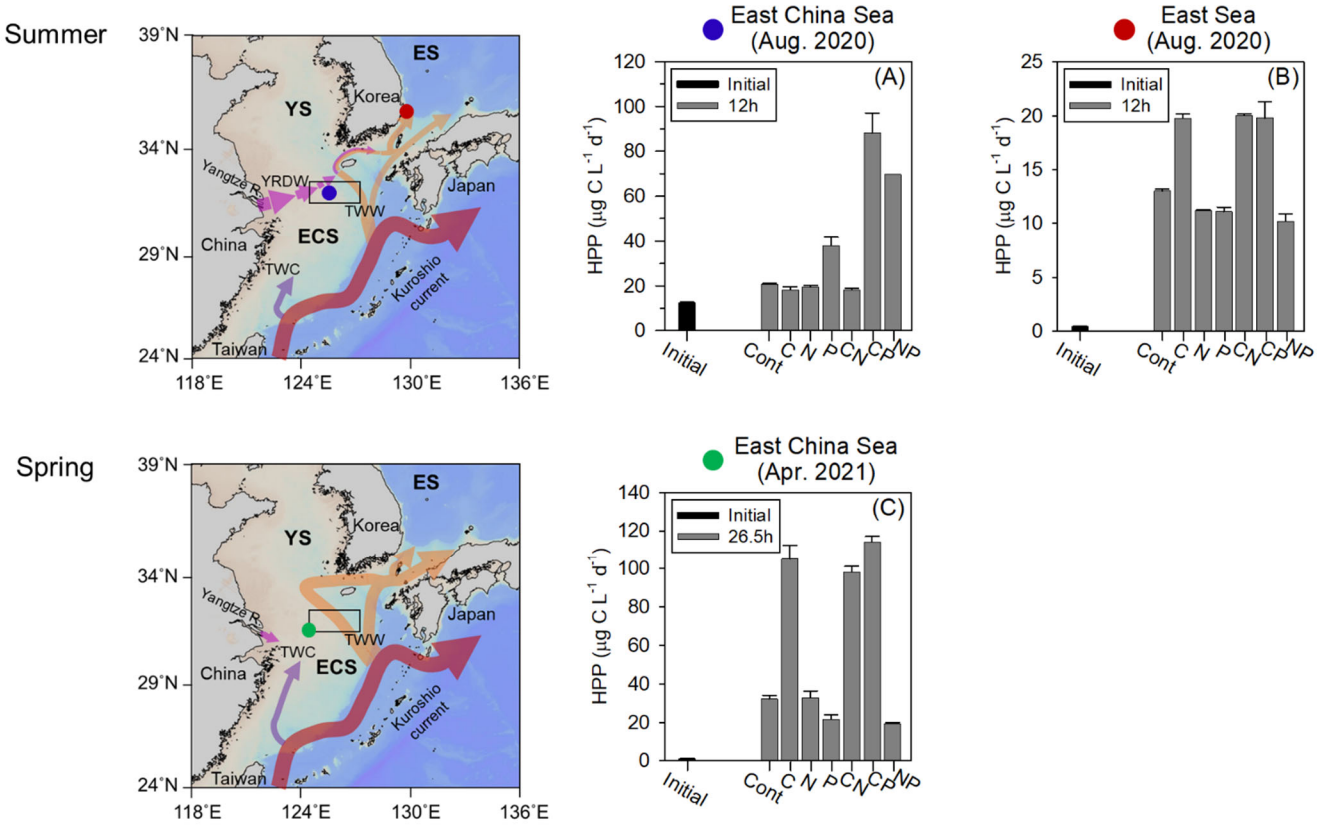

Figure 8. Maps of sampling sites where limiting resource experiments were conducted, and resource limitation of heterotrophic prokaryotes production (HPP) in the East China Sea (blue circle, A) and the East Sea (red circle, B) in August 2020, and the East China Sea (green circle, C) in April 2021. Error bars represent standard deviations. YS, Yellow Sea; ES, East Sea; ECS, East China Sea; YRDW, Yangtze River diluted water; TWC, Taiwan Warm Current; TWW, Tsushima Warm Water.

Table 2. Physico-chemical variables at the sampling depth where water samples for conducting resource-limitation experiments were collected.

	Station	Water mass	Season	Depth (m)	Temp (°C)	Salinity (psu)	DIN (μM)	DIP (μM)	N:P	DOC (μM)
Experiment 1	Northern East China Sea	YRDW	August 2020	10	28	28	4.07	0.12	33.92	91
Experiment 2	East Sea	TWW	August 2020	10	15.6	33.5	8.45	0.56	15.09	69
Experiment 3	Northern East China Sea	Kuroshio source water	April 2021	10	12.9	32.6	-	0.40	-	65

4.4 Impacts of YRDW in intensifying microbial food web

Given that the YRDW delivers high DOC but low phosphorus to the continental shelves of the ECS, it may alter substrate availability and affect the structure of both heterotrophic and autotrophic communities (Gomes et al., 2018; Kim et al., 2022), potentially leading to shifts in the relative contributions of basal producers (i.e., HP and phytoplankton) to food web dynamics and ecosystem carbon cycling. To evaluate the carbon flow through the microbial food web, we calculated the ratio of HPP to PP, representing the proportion of carbon flowing through HPP relative to PP (Fig. 9). The HPP:PP ratios observed in February and November fell within the global average 0.15 (Fig. 9A, Ducklow, 2000). However, in May, HPP:PP ranged from 0.25 to 0.53, and notably, it consistently exceeded 0.5 in August (Fig. 9A). This result indicates that the microbial food web is significantly enhanced in the nECS, especially in summer supporting a comparable amount of carbon flow through the microbial food web (Rowe et al., 2025). Notably, in August 2020, when the influence of YRDW was particularly strong, the high HPP:PP ratio (up to 0.84) is likely due to the stimulated HPP and reduced PP, resulted from increased DOC input and high turbidity, respectively (Fig. 4D, E). This suggests that climate change-induced precipitation may increasingly deliver turbid, DOC-rich, but nutrient-imbalanced freshwater to the ECS, ultimately resulting in basal production being more strongly sustained by HP than by phytoplankton, thereby driving the ECS toward a more microbially dominated food web. Such a shift could reduce the efficiency of energy transfer to higher trophic levels, potentially affecting fishery resources (Berglund et al., 2007; Rowe et al., 2025). Supporting this trend, compiled historical summer data over the past two decades revealed a gradual increase in HPP:PP ratios in the ECS (Fig. 9B). This finding suggests ongoing environmental changes, including warming and intensified precipitation events (Belkin, 2009; Khadgarai et al., 2021; Qiao et al., 2024), may increasingly shift carbon flow

toward the microbial food web rather than the classical grazing food chain. Therefore, our results highlight that YRDW runoff driven by climate change can significantly alter the trophic structure and energy transfer efficiency in the ECS, ultimately affecting fisheries by favoring smaller-sized consumers. To better understand these dynamics, further microbial oceanographic studies are needed to elucidate how YRDW influences interactions between HP parameters (i.e., respiration and carbon demand) and phytoplankton parameters (i.e., biomass and production). Such efforts are essential for assessing current ecosystem functioning and predicting future shifts in microbially mediated carbon cycling and metabolic balance (i.e., heterotrophy vs. autotrophy) in the nECS (Baek et al., in prep.).

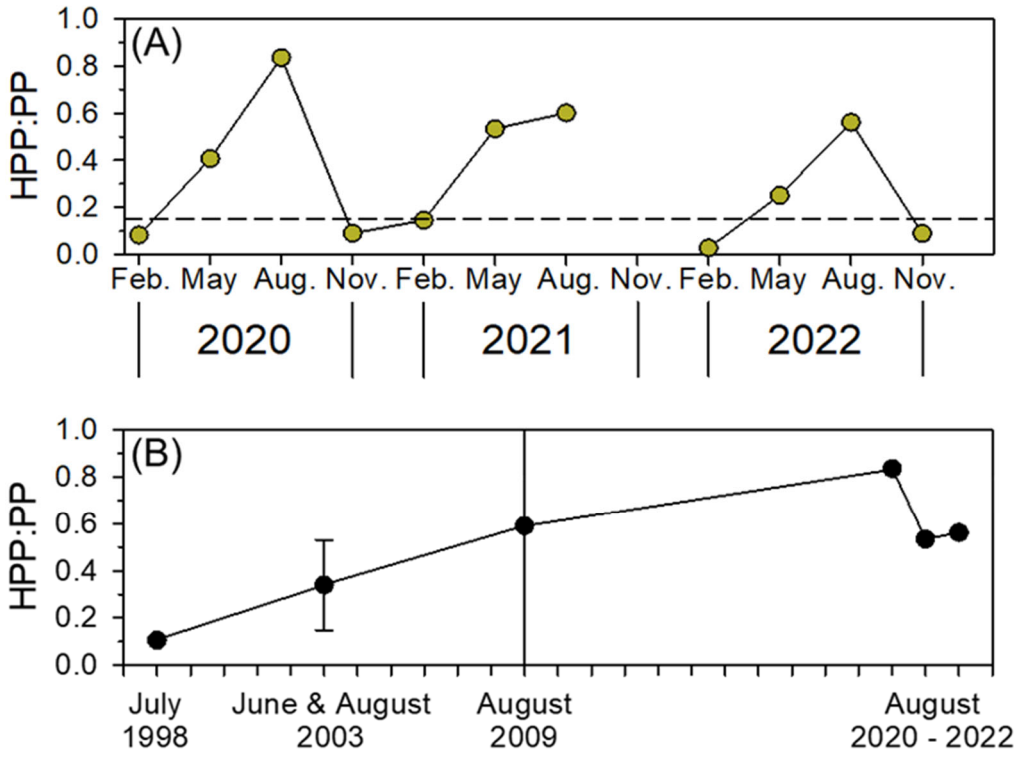

Figure 9. Seasonal variations in the ratio of heterotrophic prokaryotes production to primary production (HPP:PP) in the northern East China Sea (A), and long-term variations in HPP:PP in the ECS (B) (data adapted from Shiah et al., 2003; Chen et al., 2006; Chen et al., 2014). The horizontal dashed line indicates the global average HPP:PP ratio of 0.15 (Ducklow, 2000).

5. Conclusion

For the first time in the nECS, to our knowledge, we demonstrate that the YRDW substantially alters the concentrations and bioavailability of DOC and nutrient regimes, and thus has a significant impact on either stimulating or suppressing HPP. In general, the YRDW was a major contributor to elevated HPP in the nECS during summer by supplying DOC and stimulating high phytoplankton biomass (Fig. 5D, 6A). However, an exceptionally large-scale YRDW runoff with P-deficiency and limited DOC bioavailability rather suppressed the HPP (Fig. 7, 8). These dual contrasting impacts of YRDW, either stimulating or suppressing the HPP, partially modify the generally applicable conventional understanding that the YRDW stimulates HP activity in the ECS (Shiah et al., 2003; Chen et al., 2009).

The current ECS is undergoing drastic environmental changes resulting from rapid increases in sea surface temperature and heavy rainfall, as well as dam construction by human activities. These factors are transforming the current ECS into a different environment from what it was 10 or 20 years ago (Supplement Fig. S2, Qiao et al., 2024). For example, the P-limited condition under high YRDW input would enhance the biomass of smaller-sized phytoplankton such as cyanobacteria, small dinoflagellates, and cryptophytes (Gomes et al., 2018; Park et al., 2022), which might reduce the PP in the ECS (Gong et al., 2006; Lee et al., 2024; Fig. 4D). Consistent with this, the HPP:PP ratio has gradually increased over the past two decades (Fig. 9B), suggesting an intensifying microbial food web and shifts in ecosystem structure in the ECS. These changes imply that food web efficiency may decline, with more carbon cycled through microbial pathways rather than transferred to higher trophic levels. Such restructuring can ultimately impact the composition and productivity of fisheries. These results may also be relevant in other ocean basins that receive large terrestrial DOM inputs, and are experiencing climate warming along with increased precipitation and riverine inputs (e.g., Amazon River and Arctic Ocean).

6. Code/Data availability

The datasets collected and used in this study are publicly available from ZENODO: https://doi.org/10.5281/zenodo.18639928

7. Authors contributions:

J-HH, S-HL and S-HY conceptualized and supervised the study. Y-JB, H-KJ and BK collected samples and performed onboard experiments, as well as laboratory analyses. Y-JB, HWD, S-HK, HH and J-HH conducted data analysis and drafted the manuscript.

8. Competing interest

The contact author has declared that none of the authors has any competing interests.

9. Acknowledgements and funding

This research was supported by a grant (R2026059) from the National Institute of Fisheries Science (NIFS), funded by the Ministry of Oceans and Fisheries of Korea, by the National Research Foundation (NRF) funded by the Korean Ministry of Science and ICT (RS-2023-00275046), and by the Korea Institute of Marine Science & Technology Promotion (KIMST), funded by the Ministry of Oceans and Fisheries (RS-2025-02307311). This work was also supported by Korea Institute of Ocean Science & Technology (2520000770). The authors thank Schlitzer, Reiner, Ocean Data View, https://odv.awi.de, 2025.

10. References

Amon, R. M. W. and Benner, R.: Seasonal patterns of bacterial abundance and production in the Mississippi River plume and their importance for the fate of enhanced primary production, Microb. Ecol., 35, 289–300, https://doi.org/10.1007/s002489900084, 1998.

Azam, F., Fenchel, T., Field, J. G., Gray, J. S., Meyer-Reil, L. A., and Thingstad, F.: The ecological role of water-column microbes in the sea, Mar. Ecol. Prog. Ser., 10(3), 257–263, https://doi.org/10.3354/meps010257, 1983.

Baltar, F., Arístegui, J., Gasol, J. M., Hernández-León, S., and Herndl, G. J.: Strong coast–ocean and surface–depth gradients in prokaryotic assemblage structure and activity in a coastal transition zone region, Aquat. Microb. Ecol., 50(1), 63–74, https://doi.org/10.3354/ame01156, 2007.

Bar-On, Y. M. and Milo, R.: The biomass composition of the oceans: A blueprint of our blue planet, Cell, 179(6), 1451–1454, https://doi.org/10.1016/j.cell.2019.11.018, 2019.

Belkin, I. M.: Rapid warming of large marine ecosystems, Prog. Oceanogr., 81(1–4), 207–213, https://doi.org/10.1016/j.pocean.2009.04.011, 2009.

Berglund, J., Müren, U., Båmstedt, U., and Andersson, A.: Efficiency of a phytoplankton-based and a bacterial-based food web in a pelagic marine system, Limnol. Oceanogr., 52, 121–131, https://doi.org/10.4319/lo.2007.52.1.0121, 2007.

Cao, S., Sun, F., Lu, D., and Zhou, Y.: Characterization of refractory dissolved organic matter (rDOM) in sludge alkaline fermentation liquid driven denitrification: Effect of HRT on their fate and transformation, Water Res., 159, 135–144, https://doi.org/10.1016/j.watres.2019.04.063, 2019.

Carlson, C. A. and Hansell, D. A.: DOM sources, sinks, reactivity, and budgets, in: Biogeochemistry of Marine Dissolved Organic Matter, 2nd Edn., edited by: Hansell, D. A. and Carlson, C. A., Academic Press, 65–126, https://doi.org/10.1016/B978-0-12-405940-5.00003-0, 2015.

Carlson, C. A., del Giorgio, P. A., and Herndl, G. J.: Microbes and the dissipation of energy and respiration: From cells to ecosystems, Oceanography, 20(2), 89–100, https://doi.org/10.5670/oceanog.2007.52, 2007.

Chang, P.-H. and Isobe, A.: A numerical study on the Changjiang diluted water in the Yellow and East China Seas, J. Geophys. Res., 108, 3299, https://doi.org/10.1029/2002JC001749, 2003.

Chen, B., Huang, B., Xie, Y., Guo, C., Song, S., Li, H., and Liu, H.: The bacterial abundance and production in the East China Sea: seasonal variations and relationships with the phytoplankton biomass and production, Acta Oceanol. Sin., 33, 166–177, https://doi.org/10.1007/s13131-014-0528-0, 2014.

Chen, C.-C., Chiang, K.-P., Gong, G.-C., Shiah, F.-K., Tseng, C.-M., and Liu, K.-K.: Importance of planktonic community respiration on the carbon balance of the East China Sea in summer, Global Biogeochem. Cy., 20, GB4001, https://doi.org/10.1029/2005GB002647, 2006.

Chen, C.-C., Gong, G.-C., Chiang, K.-P., Shiah, F.-K., Chung, C.-C., and Hung, C.-C.: Scaling effects of a eutrophic river plume on organic carbon consumption, Limnol. Oceanogr., 66, 1867–1881, https://doi.org/10.1002/lno.11729, 2021.

Chen, C.-C., Shiah, F.-K., Chiang, K.-P., Gong, G.-C., and Kemp, W. M.: Effects of the Changjiang (Yangtze) River discharge on planktonic community respiration in the East China Sea, J. Geophys. Res., 114, C03005, https://doi.org/10.1029/2008JC004891, 2009.

Chen, J., Li, D., Jin, H., Jiang, Z., Wang, B., Wu, B., Hao, Q., and Sun, X.: Changing nutrients, oxygen and phytoplankton in the East China Sea, in: Changing Asia-Pacific Marginal Seas, Atmosphere, Earth, Ocean & Space, edited by: Chen, C.-T. A. and Guo, X., Springer, Singapore, 155–170, https://doi.org/10.1007/978-981-15-4886-4_10, 2020.

Chen, Z. L., Zhang, H., Yi, Y., He, Y., Li, P., Wang, Y., Wang, K., Yan, Z., He, C., Shi, Q., and He, D.: Dissolved organic matter composition and characteristics during extreme flood events in the Yangtze River Estuary, Sci. Total Environ., 914, 169827, https://doi.org/10.1016/j.scitotenv.2023.169827, 2024.

Coble, P. G.: Characterization of marine and terrestrial DOM in seawater using excitation-emission matrix spectroscopy, Mar. Chem., 51, 325–346, https://doi.org/10.1016/0304-4203(95)00062-3, 1996.

del Giorgio, P. A., Cole, J. J., and Cimbleris, A.: Respiration rates in bacteria exceed phytoplankton production in unproductive aquatic systems, Nature, 385, 148–151, https://doi.org/10.1038/385148a0, 1997.

Dickman, E. M., Newell, J. M., González, M. J., and Vanni, M. J.: Light, nutrients, and food-chain length constrain planktonic energy transfer efficiency across multiple trophic levels, Proc. Natl. Acad. Sci. USA, 105(47), 18408–18412, https://doi.org/10.1073/pnas.0805566105, 2008.

Dittmar, T., Lennartz, S. T., Buck-Wiese, H., Hansell, D. A., Santinelli, C., Vanni, C., Blasius, B., and Hehemann, J.-H.: Enigmatic persistence of dissolved organic matter in the ocean, Nat. Rev. Earth Environ., 2, 570–583, https://doi.org/10.1038/s43017-021-00183-7, 2021.

Drakare, S.: Competition between picoplanktonic cyanobacteria and heterotrophic bacteria along crossed gradients of glucose and phosphate, Microb. Ecol., 44, 327–335, https://doi.org/10.1007/s00248-002-1013-4, 2002.

Ducklow, H. W. and Carlson, C. A.: Oceanic bacterial production, in: Advances in Microbial Ecology, vol. 12, edited by: Marshall, K. C., Springer, Boston, MA, USA, 113–181, https://doi.org/10.1007/978-1-4684-7609-5_3, 1992.

Ducklow, H.: Bacterial production and biomass in the oceans, in: Microbial Ecology of the Oceans, edited by: Kirchman, D. L., Wiley, Hoboken, USA, 85–120, 2000.

Fagerbakke, K. M., Heldal, M., and Norland, S.: Content of carbon, nitrogen, oxygen, sulfur, and phosphorus in native aquatic and cultured bacteria, Aquat. Microb. Ecol., 10, 15–27, https://doi.org/10.3354/ame010015, 1996.

Fasching, C., Behounek, B., Battin, T. J., and Ulseth, K. J.: Microbial degradation of terrigenous dissolved organic matter and potential consequences for carbon cycling in brown-water streams, Sci. Rep., 4, 4981, https://doi.org/10.1038/srep04981, 2014.

Ferguson, R. L., Buckley, E. N., and Palumbo, A. V.: Response of marine bacterioplankton to differential filtration and confinement, Appl. Environ. Microbiol., 47, 49–55, https://doi.org/10.1128/aem.47.1.49-55.1984, 1984.

Fernandes, V. and Bogati, K.: Analysis of bacteria–phytoplankton relationships at three discrete locations in the Eastern Arabian Sea during winter, Cont. Shelf Res., 243, 104751, https://doi.org/10.1016/j.csr.2022.104751, 2022.

Ferrera, I., Sebastian, M., Acinas, S. G., and Gasol, J. M.: Prokaryotic functional gene diversity in the sunlit ocean: Stumbling in the dark, Curr. Opin. Microbiol., 25, 33–39, https://doi.org/10.1016/j.mib.2015.03.007, 2015.

Fujibe, F., Yamazaki, N., and Kobayashi, K.: Long-term changes in the diurnal precipitation cycles in Japan for 106 years (1898–2003), J. Meteorol. Soc. Jpn., 84, 311–317, https://doi.org/10.2151/jmsj.84.311, 2006.

Gasol, J. M., del Giorgio, P. A., and Duarte, C. M.: Biomass distribution in marine planktonic communities, Limnol. Oceanogr., 42, 1353–1363, https://doi.org/10.4319/lo.1997.42.6.1353, 1997.

Goldman, J. C., Caron, D. A., and Dennett, M. R.: Regulation of gross growth efficiency and ammonium regeneration in bacteria by substrate C:N ratio, Limnol. Oceanogr., 32, 1239–1252, https://doi.org/10.4319/lo.1987.32.6.1239, 1987.

Gomes, A., Gasol, J. M., Estrada, M., Franco-Vidal, L., Díaz-Pérez, L., Ferrera, I., and Morán, X. A. G.: Heterotrophic bacterial responses to the winter–spring phytoplankton bloom in open waters of the NW Mediterranean, Deep-Sea Res. Pt. I, 96, 59–68, https://doi.org/10.1016/j.dsr.2014.11.007, 2015.

Gomes, H. R., Xu, Q., Ishizaka, J., Carpenter, E. J., Yager, P. L., and Goes, J. I.: The influence of riverine nutrients in niche partitioning of phytoplankton communities: A contrast between the Amazon River plume and the Changjiang River diluted water of the East China Sea, Front. Mar. Sci., 5, 343, https://doi.org/10.3389/fmars.2018.00343, 2018.

Gong, G.-C., Chang, J., Chiang, K.-P., Hsiung, T.-M., Hung, C.-C., Duan, S.-W., and Codispoti, L. A.: Reduction of primary production and changing of nutrient ratio in the East China Sea: Effect of the Three Gorges Dam?, Geophys. Res. Lett., 33, L07610, https://doi.org/10.1029/2006GL025800, 2006.

Gong, G. C., Lee Chen, Y. L., and Liu, K. K.: Chemical hydrography and chlorophyll a distribution in the East China Sea in summer: Implications in nutrient dynamics, Cont. Shelf Res., 16, 1561–1590, https://doi.org/10.1016/0278-4343(96)00005-2, 1996.

Guo, W., Yang, L., Zhai, W., Chen, W., Osburn, C. L., Huang, X., and Li, Y.: Runoff-mediated seasonal oscillation in the dynamics of dissolved organic matter in different branches of a large bifurcated estuary – The Changjiang Estuary, J. Geophys. Res.-Biogeo., 119, 776–793, https://doi.org/10.1002/2013JG002540, 2014.

Hama, T., Miyazaki, T., Ogawa, Y., Iwakuma, T., Takahashi, M., Otsuki, A., and Ichimura, S.: Measurement of photosynthetic production of a marine phytoplankton population using a stable ^{13}C isotope, Mar. Biol., 73, 31–36, https://doi.org/10.1007/BF00396282, 1983.

Hansen, A. M., Kraus, T. E. C., Pellerin, B. A., Fleck, J. A., Downing, B. D., and Bergamaschi, B. A.: Optical properties of dissolved organic matter (DOM): Effects of biological and photolytic degradation, Limnol. Oceanogr., 61, 1015–1032, https://doi.org/10.1002/lno.10270, 2016.

Huguet, A., Vacher, L., Relexans, S., Saubusse, S., Froidefond, J. M., and Parlanti, E.: Properties of fluorescent dissolved organic matter in the Gironde Estuary, Org. Geochem., 40, 706–719, https://doi.org/10.1016/j.orggeochem.2009.03.002, 2009.

Hur, H. B., Jacobs, G. A., and Teague, W. J.: Monthly variations of water masses in the Yellow and East China Seas, November 6, 1998, J. Oceanogr., 55, 171–184, 1999.

Hyun, J.-H. and Yang, E. J.: Freezing seawater for the long-term storage of bacterial cells for microscopic enumeration, J. Microbiol., 41, 262–265, 2003.

Hyun, J.-H. and Yang, E. J.: Meso-scale spatial variation in bacterial abundance and production associated with surface convergence and divergence in the NE equatorial Pacific, Aquat. Microb. Ecol., 41, 1–13, https://doi.org/10.3354/ame041001, 2005.

Hyun, J.-H., Kim, D., Shin, C.-W., Noh, J.-H., Yang, E.-J., Mok, J.-S., Kim, S.-H., Kim, H.-C., and Yoo, S.: Enhanced phytoplankton and bacterioplankton production coupled to coastal upwelling and an anticyclonic eddy in the Ulleung Basin, East Sea, Aquat. Microb. Ecol., 54, 45–54, https://doi.org/10.3354/ame01280, 2009.

Hyun, J.-H., Kim, S.-H., Yang, E. J., Choi, A., and Lee, S. H.: Biomass, production, and control of heterotrophic bacterioplankton during a late phytoplankton bloom in the Amundsen Sea Polynya, Antarctica, Deep-Sea Res. Pt. II, 123, 102–112, https://doi.org/10.1016/j.dsr2.2015.10.001, 2016.

Jiang, Y., Zhao, J., Li, P., and Huang, Q.: Linking optical properties of dissolved organic matter to multiple processes at the coastal plume zone in the East China Sea, Environ. Sci.-Proc. Impacts, 18(10), 1316–1324, https://doi.org/10.1039/C6EM00341A, 2016.

Jiao, N., Herndl, G. J., Hansell, D. A., Benner, R., Kattner, G., Wilhelm, S. W., Kirchman, D. L., Weinbauer, M. G., Luo, T., Chen, F., and Azam, F.: Microbial production of recalcitrant dissolved organic matter: Long-term carbon storage in the global ocean, Nat. Rev. Microbiol., 8, 593–599, https://doi.org/10.1038/nrmicro2386, 2010.

Joint, I., Henriksen, P., Fonnes, G. A., Bourne, D., Thingstad, T. F., and Riemann, B.: Competition for inorganic nutrients between phytoplankton and bacterioplankton in nutrient manipulated mesocosms, Aquat. Microb. Ecol., 29(2), 145–159, https://doi.org/10.3354/ame029145, 2002.

JPL.: JPL CAP SMAP Sea Surface Salinity Products Ver. 5.0, PO.DAAC, CA, USA. Dataset accessed [2024-01-30] at https://doi.org/10.5067/SMP50-3TPCS, 2020.

Karl, D. M.: Microbial oceanography: paradigms, processes and promise, Nat. Rev. Microbiol., 5, 759–769, https://doi.org/10.1038/nrmicro1749, 2007.

Khadgarai, S., Kumar, V., and Pradhan, P. K.: The connection between extreme precipitation variability over monsoon Asia and large-scale circulation patterns, Atmosphere, 12(11), 1492, https://doi.org/10.3390/atmos12111492, 2021.

Kim, B. and Youn, S.-H.: Spatial distribution of heterotrophic bacteria and the role of microbial food web in the northern East China Sea in summer, Environ. Biol. Res., 41, 89–100, https://doi.org/10.11626/kjeb.2023.41.1.089, 2023.

Kim, B., An, S. U., Kim, T. H., and Hyun, J.-H.: Uncoupling between heterotrophic bacteria and phytoplankton and changes in trophic balance associated with warming of seawater in Gyeonggi Bay, Yellow Sea, Estuaries Coasts, 43, 535–546, https://doi.org/10.1007/s12237-019-00606-1, 2020.

Kim, B., Baek, Y.-J., Han, H., Lee, H., Youn, S.-H., and Hyun, J.-H.: P-limited prokaryotic heterotrophic production and metabolic balance between prokaryotic carbon demand and phytoplankton primary production in summer in the central Yellow Sea, Ocean Sci. J., 60, 14, https://doi.org/10.1007/s12601-025-00209-x, 2025.

Kim, D., Choi, S. H., Shim, J., Kim, K. H., and Kim, C. H.: Revisiting the seasonal variations of sea–air CO_2 fluxes in the northern East China Sea, Terr. Atmos. Ocean. Sci., 24(3), https://doi.org/10.3319/TAO.2012.12.06.01(OC), 2013a.

Kim, H. R., Lim, J. H., Kim, J. H., Thangaraj, S., and Kim, I. N.: Physical process controlling the surface bacterial community composition in the Ulleung Basin of East Sea, Front. Mar. Sci., 9, 841492, https://doi.org/10.3389/fmars.2022.841492, 2022.

Kim, J.-Y., Yoon, M.-G., Moon, C.-H., Gang, C.-G., Choi, K., and Lee, C. I.: Morphological and genetic stock identification of *Todarodes pacificus* in Korean waters, J. Korean Soc. Oceanogr., 18(3), 131–141, https://doi.org/10.7850/JKSO.2013.18.3.131, 2013b.

Kirchman, D. L.: Leucine incorporation as a measure of biomass production by heterotrophic bacteria, in: Handbook of Methods in Aquatic Microbial Ecology, edited by: Kemp, P. F., Sherr, B. F., Sherr, E. B., and Cole, J. J., Lewis Publishers, Boca Raton, USA, 700–709, 1993.

Kragh, T. and Søndergaard, M.: Production and decomposition of new DOC by marine plankton communities: Carbohydrates, refractory components and nutrient limitation, Biogeochemistry, 96, 177–187, https://doi.org/10.1007/s10533-009-9357-1, 2009.

Kritzberg, E. S., Arrieta, J. M., and Duarte, C. M.: Temperature and phosphorus regulating carbon flux through bacteria in a coastal marine system, Aquat. Microb. Ecol., 58, 141–151, https://doi.org/10.3354/ame01368, 2010.

Lee, D., Lee, D.-H., Joo, H., Jang, H. K., Park, S., Kim, Y., Kim, S., Kim, J., Kim, M., Kwon, J.-I., and Lee, S.: Long-term variability of phytoplankton primary production in the Ulleung Basin, East Sea/Japan Sea using ocean color remote sensing, J. Geophys. Res.-Oceans, 129, e2024JC020898, https://doi.org/10.1029/2024JC020898, 2024.

Lemée, R., Rochelle-Newall, E., Van Wambeke, F., Pizay, M.-D., Rinaldi, P., and Gattuso, J.-P.: Seasonal variation of bacterial production, respiration and growth efficiency in the open NW Mediterranean Sea, Aquat. Microb. Ecol., 29, 227–237, https://doi.org/10.3354/ame029227, 2002.

Li, G., Han, X., Yue, S., Wen, G., Rongmin, Y., and Kusky, T. M.: Monthly variations of water masses in the East China Seas, Cont. Shelf Res., 26, 1954–1970, https://doi.org/10.1016/j.csr.2006.06.005, 2006.

Li, K., Liu, C., Ma, Y., and Wang, X.: Land-based dissolved organic nitrogen dynamics and bioavailability in Jiaozhou Bay, China, Estuar. Coast. Shelf Sci., 220, 13–24, https://doi.org/10.1016/j.ecss.2019.02.045, 2019a.

Li, P., Chen, L., Zhang, W., and Huang, Q.: Spatiotemporal distribution, sources, and photobleaching imprint of dissolved organic matter in the Yangtze Estuary and its adjacent sea using fluorescence and parallel factor analysis, PLOS ONE, 10(6), e0130852, https://doi.org/10.1371/journal.pone.0130852, 2015.

Li, Y., Xu, C., Zhang, W., Lin, L., Wang, L., Niu, L., Zhang, H., Wang, P., and Wang, C.: Response of bacterial community in composition and function to the various DOM at river confluences in the urban area, Water Res., 169, 115293, https://doi.org/10.1016/j.watres.2019.115293, 2020.

Li, Z., Sun, Y., Li, T., Ding, Y., and Hu, T.: Future changes in East Asian summer monsoon circulation and precipitation under 1.5 to 5 °C of warming, Earth's Future, 7, 1391–1406, https://doi.org/10.1029/2019EF001276, 2019b.

Lie, H.-J. and Cho, C.-H.: Seasonal circulation patterns of the Yellow and East China Seas derived from satellite-tracked drifter trajectories and hydrographic observations, Prog. Oceanogr., 146, 121–141, https://doi.org/10.1016/j.pocean.2016.06.004, 2016.

Lopez, P., Lluch, X., Vidal, M., and Morguí, J. A.: Adsorption of phosphorus on sediments of the Balearic Islands (Spain) related to their composition, Estuar. Coast. Shelf Sci., 42, 185–196, https://doi.org/10.1006/ecss.1996.0014, 1996.

Mann, K. H. and Lazier, J. R. N.: Dynamics of Marine Ecosystems: Biological–Physical Interactions in the Oceans, 3rd Edn., Blackwell Publishing Ltd., Oxford, UK, https://doi.org/10.1002/9781118687901, 2005.

Milliman, J. D. and Farnsworth, K. L.: River Discharge to the Coastal Ocean: A Global Synthesis, Cambridge Univ. Press, Cambridge, UK, 16–61, https://doi.org/10.1017/CBO9780511781247, 2013.

Min, J.-O., Kim, S.-H., Jung, J., Jung, U.-J., Yang, E. J., Lee, S., and Hyun, J.-H.: Glacial ice melting stimulates heterotrophic prokaryotes production on the Getz Ice Shelf in the Amundsen Sea, Antarctica, Geophys. Res. Lett., 49, e2021GL097627, https://doi.org/10.1029/2021GL097627, 2022.

Nam, S., Wu, Y., Hwang, J., Rykaczewski, R. R., and Kim, G.: Editorial: Physics and biogeochemistry of the East Asian marginal seas, Front. Mar. Sci., 9, 945814, https://doi.org/10.3389/fmars.2022.945814, 2022.

Obernosterer, I., Kawasaki, N., and Benner, R.: P-limitation of respiration in the Sargasso Sea and uncoupling of bacteria from P-regeneration in size-fractionation experiments, Aquat. Microb. Ecol., 32, 229–237, https://doi.org/10.3354/ame032229, 2003.

Park, K.-W., Oh, H.-J., Moon, S.-Y., Yoo, M.-H., and Youn, S.-H.: Effects of miniaturization of the summer phytoplankton community on the marine ecosystem in the northern East China Sea, J. Mar. Sci. Eng., 10, 315, https://doi.org/10.3390/jmse10030315, 2022.

Poole, H. H. and Atkins, W. R. G.: Photo-electric measurements of submarine illumination throughout the year, J. Mar. Biol. Assoc. UK, 16, 297–324, https://doi.org/10.1017/S0025315400029829, 1929.

Porter, K. G. and Feig, Y. S.: The use of DAPI for identifying and counting aquatic microflora, Limnol. Oceanogr., 25, 943–948, https://doi.org/10.4319/lo.1980.25.5.0943, 1980.

Puddu, A., Zoppini, A., Fazi, S., Rosati, M., Amalfitano, S., and Magaletti, E.: Bacterial uptake of DOM released from P-limited phytoplankton, FEMS Microbiol. Ecol., 46(3), 257–268, https://doi.org/10.1016/S0168-6496(03)00197-1, 2003.

Qiao, Y.-X., Nakamura, H., and Tomita, T.: Warming of the Kuroshio Current over the last four decades has intensified the Meiyu-Baiu rainband, Geophys. Res. Lett., 51, e2023GL107021, https://doi.org/10.1029/2023GL107021, 2024.

Rebstock, G. A. and Kang, Y. S.: A comparison of three marine ecosystems surrounding the Korean peninsula: Responses to climate change, Prog. Oceanogr., 59, 357–379, https://doi.org/10.1016/j.pocean.2003.10.002, 2003.

Remote Sensing Systems (RSS).: SMAP Sea Surface Salinity Products. Ver. 4.0, PO.DAAC, CA, USA. Dataset accessed [2024-01-30] at https://doi.org/10.5067/SMP40-3SMCS, 2019

Rivkin, R. B. and Anderson, M. R.: Inorganic nutrient limitation of oceanic bacterioplankton, Limnol. Oceanogr., 42, 730–740, https://doi.org/10.4319/lo.1997.42.4.0730, 1997.

Robinson, C. and Williams, P. J. le B.: Temperature and Antarctic plankton community respiration, J. Plankton Res., 15, 1035–1051, https://doi.org/10.1093/plankt/15.9.1035, 1993.

Rowe, O. F., Paczkowska, J., Brutemark, A., Brugel, S., Traving, S. J., Lefébure, R., Miranda, F., Guleikova, L., Griniene, E., Jurgensone, I., Byström, P., Riemann, L., and Andersson, A.: Climate change–induced terrestrial matter runoff may decrease food web production in coastal ecosystems, Limnol. Oceanogr., https://doi.org/10.1002/lno.12762, 2025.

Seo, J., Kim, G., and Hwang, J.: Sources and behavior of particulate organic carbon in the Yellow Sea and the East China Sea based on ^{13}C, ^{14}C, and ^{234}Th, Front. Mar. Sci., 9, 793556, https://doi.org/10.3389/fmars.2022.793556, 2022.

Shi, G., Peng, C., Wang, M., Shi, S., Yang, Y., Chu, J., Zhang, J., Lin, G., Shen, Y., and Zhu, Q.: The spatial and temporal distribution of dissolved organic carbon exported from three Chinese rivers to the China Sea, PLOS ONE, 11, e0165039, https://doi.org/10.1371/journal.pone.0165039, 2016.

Shiah, F.-K., Gong, G.-C., and Chen, C.-C.: Seasonal and spatial variation of bacterial production in the continental shelf of the East China Sea: Possible controlling mechanisms and potential roles in carbon cycling, Deep-Sea Res. Pt. II, 50, 1295–1309, https://doi.org/10.1016/S0967-0645(03)00024-9, 2003.

Smith, D. C. and Azam, F.: A simple, economical method for measuring bacterial protein synthesis rates in seawater using ^{3}H-leucine, Mar. Microb. Food Webs, 6, 107–114, 1992.

Spielhagen, R. F. and Bauch, H. A.: The role of Arctic Ocean freshwater during the past 200 ky, Arktos, 1, 18, https://doi.org/10.1007/s41063-015-0013-9, 2015.

Stedmon, C. A. and Bro, R.: Characterizing dissolved organic matter fluorescence with parallel factor analysis: A tutorial, Limnol. Oceanogr.-Methods, 6, 572–579, https://doi.org/10.4319/lom.2008.6.572, 2008.

Straile, D.: Gross growth efficiencies of protozoan and metazoan zooplankton and their dependence on food concentration, predator–prey weight ratio, and taxonomic group, Limnol. Oceanogr., 42, 1375–1385, https://doi.org/10.4319/lo.1997.42.6.1375, 1997.

Thingstad, T. F., Krom, M. D., Mantoura, R. F. C., Flaten, G. A. F., Groom, S., Herut, B., Kress, N., Law, C. S., Pasternak, A., Pitta, P., Psarra, S., Rassoulzadegan, F., Tanaka, T., Tselepides, A., Wassmann, P., Woodward, E. M. S., Wexels Riser, C., Zodiatis, G., and Zohary, T.: Nature of phosphorus limitation in the ultraoligotrophic eastern Mediterranean, Science, 309, 1068–1071, https://doi.org/10.1126/science.1112632, 2005.

Wang, H., Yan, H., Zhou, F., Li, B., Zhuang, W., and Yang, Y.: Dynamics of nutrient export from the Yangtze River to the East China Sea, Estuar. Coast. Shelf Sci., 229, 106415, https://doi.org/10.1016/j.ecss.2019.106415, 2019.

Wang, S.-L., Chen, C.-T. A., Hong, G.-H., and Chung, C.-S.: Carbon dioxide and related parameters in the East China Sea, Cont. Shelf Res., 20(4–5), 525–544, https://doi.org/10.1016/S0278-4343(99)00084-9, 2000.

White, P. A., Kalff, J., Rasmussen, J. B., and Gasol, J. M.: The effect of temperature and algal biomass on bacterial production and specific growth rate in freshwater and marine habitats, Microb. Ecol., 21, 99–118, https://doi.org/10.1007/BF02539147, 1991.

Yamashita, Y. and Tanoue, E.: Production of bio-refractory fluorescent dissolved organic matter in the ocean interior, Nat. Geosci., 1, 579–582, https://doi.org/10.1038/ngeo279, 2008.

Yoon, S. C., Youn, S. H., Whang, J. D., Suh, Y. S., and Yoon, Y. Y.: Long-term variation in ocean environmental conditions of the northern East China Sea, J. Korean Soc. Mar. Environ. Energy, 18, 189–206, https://doi.org/10.7846/JKOSMEE.2015.18.3.189, 2015.

Yuan, X., Yin, K., Harrison, P. J., He, L., and Xu, J.: Variations in apparent oxygen utilization and effects of P addition on bacterial respiration in subtropical Hong Kong waters, Estuaries Coasts, 34, 536–543, https://doi.org/10.1007/s12237-010-9329-7, 2011.

Zhao, S., Xiao, T., Lu, R., and Lin, Y.: Spatial variability in biomass and production of heterotrophic bacteria in the East China Sea and the Yellow Sea, Deep-Sea Res. Pt. II, 57, 1071–1078, https://doi.org/10.1016/j.dsr2.2010.02.009, 2010.